Title
A quantitative assessment of distributions and sources of tropospheric halocarbons measured in Singapore

Authors
Sarkar, Sayantan
Fan, Wei Hong
Jia, Shiguo
et al.

Publication Date
2018-04-01

DOI
10.1016/j.scitotenv.2017.11.087

Science of the Total Environment 619–620 (2018) 528–544

Contents lists available at ScienceDirect

Science of the Total Environment

journal homepage: www.elsevier.com/locate/scitotenv

A quantitative assessment of distributions and sources of tropospheric halocarbons measured in Singapore

Sayantan Sarkar [a,*], Wei Hong Fan [b], Shiguo Jia [b,1], Donald R. Blake [c], Jeffrey S. Reid [d], Puji Lestari [e], Liya E. Yu [a,b]

[a] NUS Environmental Research Institute, National University of Singapore, 5A Engineering Drive 1, Singapore 117411, Singapore
[b] Department of Civil and Environmental Engineering, National University of Singapore, 1 Engineering Drive 2, Singapore 117576, Singapore
[c] Department of Chemistry, University of California, 1102 Natural Sciences 2, Irvine, CA 92697-2025, USA
[d] Naval Research Laboratory, Marine Meteorology Division, 7 Grace Hopper Avenue Stop 2, Monterey, CA 93943-5502, USA
[e] Environmental Engineering Department, Institut Teknologi Bandung, JL. Ganesha No. 10, Bandung 40132, Indonesia

HIGHLIGHTS

- First ground-based atmospheric measurements of 26 halocarbons in Southeast Asia
- Montreal Protocol regulated species are close to global backgrounds.
- Chlorofluorocarbon replacements show significant enhancements above baseline.
- Transported peat-forest burning smoke affects selected short-lived halocarbons.

GRAPHICAL ABSTRACT

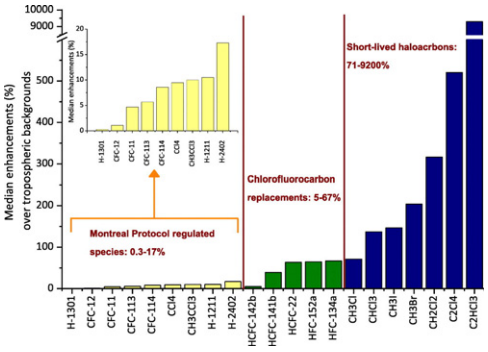

ARTICLE INFO

Article history:
Received 23 May 2017
Received in revised form 19 October 2017
Accepted 8 November 2017
Available online 29 November 2017

Editor: P. Kassomenos

Keywords:
Chlorofluorocarbons (CFCs)
Hydrochlorofluorocarbons (HCFCs)
Short-lived halocarbons
Montreal Protocol
Positive matrix factorization (PMF)
Southeast Asia

ABSTRACT

This work reports the first ground-based atmospheric measurements of 26 halocarbons in Singapore, an urban-industrial city-state in Southeast (SE) Asia. A total of 166 whole air canister samples collected during two intensive 7 Southeast Asian Studies (7SEAS) campaigns (August–October 2011 and 2012) were analyzed for C_1-C_2 halocarbons using gas chromatography-electron capture/mass spectrometric detection. The halocarbon dataset was supplemented with measurements of selected non-methane hydrocarbons (NMHCs), C_1-C_5 alkyl nitrates, sulfur gases and carbon monoxide to better understand sources and atmospheric processes. The median observed atmospheric mixing ratios of CFCs, halons, CCl_4 and CH_3CCl_3 were close to global tropospheric background levels, with enhancements in the 1–17% range. This provided the first measurement evidence from SE Asia of the effectiveness of Montreal Protocol and related national-scale regulations instituted in the 1990s to phase-out ozone depleting substances (ODS). First- and second-generation CFC replacements (HCFCs and HFCs) dominated the atmospheric halocarbon burden with HFC-134a, HCFC-22 and HCFC-141b exhibiting enhancements of 39–67%. By combining near-source measurements in Indonesia with receptor data in Singapore, regionally transported peat-forest burning smoke was found to impact levels of several NMHCs (ethane, ethyne, benzene, and propane) and short-lived halocarbons (CH_3I, CH_3Cl, and CH_3Br) in a subset of the receptor samples. The strong signatures of these species near peat-forest fires were potentially affected by atmospheric dilution/mixing during transport

* Corresponding author currently at: Department of Earth Sciences and Centre for Climate and Environmental Studies, Indian Institute of Science Education and Research (IISER) – Kolkata, Mohanpur, 741246 Nadia, West Bengal, India.
E-mail address: sayantan.sarkar@iiserkol.ac.in (S. Sarkar).
[1] Currently at: School of Atmospheric Sciences, and Guangdong Province Key Laboratory for Climate Change and Natural Disaster Studies, Sun Yat-sen University, Guangzhou 510275, People's Republic of China.

https://doi.org/10.1016/j.scitotenv.2017.11.087

and by mixing with substantial urban/regional backgrounds at the receptor. Quantitative source apportionment was carried out using positive matrix factorization (PMF), which identified industrial emissions related to refrigeration, foam blowing, and solvent use in chemical, pharmaceutical and electronics industries as the major source of halocarbons (34%) in Singapore. This was followed by marine and terrestrial biogenic activity (28%), residual levels of ODS from pre-Montreal Protocol operations (16%), seasonal incidences of peat-forest smoke (13%), and fumigation related to quarantine and pre-shipment (QPS) applications (7%).

1. Introduction

Chlorofluorocarbons (CFCs) and their first- and second-generation replacement products, hydrochlorofluorocarbons (HCFCs) and hydrofluorocarbons (HFCs), are entirely anthropogenic in origin and were developed in the 1930s and continued evolving through the 1980s for domestic and industrial applications as refrigerants, solvents, propellants, and foam blowing agents. Because of their chemical inertness, the only realistic sink mechanism of tropospheric CFCs upon their release is transport to the stratosphere. Here, CFCs are photolyzed by UV radiation producing Cl atoms that catalytically destroy stratospheric O_3 (Kim et al., 2011 and references therein). Halons, a separate group of bromine-containing halocarbons primarily used as fire suppression agents, undergo similar troposphere-stratosphere transport. This is followed by photolytic production of Br, which is more efficient than Cl on a per-atom basis in destroying stratospheric O_3. Consequently, halons are known to have higher ozone depletion potentials (ODP) as compared to CFCs. In contrast, HCFCs and HFCs are partially removed in the troposphere upon reaction with OH, and are less significant contributors to stratospheric O_3 depletion (Kim et al., 2011). Overall, O_3 depletion since the 1970s, primarily attributed to these ozone depleting substances (ODS), is estimated to contribute a non-trivial globally averaged radiative forcing (RF) of -0.15 ± 0.10 W m^{-2} (IPCC/TEAP, 2005). In addition, these halocarbons exert a considerable influence on global direct radiative forcing owing to their ability to absorb long-wave (IR) radiation and their long atmospheric lifetimes (on the order of decades to centuries). Global increases in industrially produced ODS and non-ODS halocarbons from 1750 to 2000 are estimated to exert a positive RF of $+0.33 \pm 0.03$ W m^{-2}, corresponding to ~13% of the total RF exhibited by all greenhouses gases (IPCC/TEAP, 2005).

In view of the environmental impacts described above, the production and use of these and other ODS such as CCl_4 and CH_3CCl_3 were regulated by the Montreal Protocol (MP) in 1989 and its subsequent amendments, imposing a complete ban on CFCs for developed and developing countries by 1996 and 2010, respectively. On the other hand, HCFCs are allowed to undergo step-wise reduction between 2004 and 2030 for developed countries and between 2013 and 2040 for developing countries (Keller et al., 2012). In the post-MP era, long-term ground-based measurements at remote locations have reported gradually decreasing or stabilizing trends for tropospheric CFCs, CCl_4 and CH_3CCl_3 (Prinn et al., 2016; ESRL, 2016), showing the general effectiveness of the global phase-out of these ODS. However, such trends insufficiently reflect the effectiveness of MP regulations at a regional scale or in individual countries where information on halocarbons is mostly derived based on national or regional bottom-up emission inventories. These inventories could have inherent uncertainties arising from inaccuracies in assigning halocarbon usage data among end-use sectors based on production data, overlooked leakage from existing stockpiles, and unreported production (Fang et al., 2012 and references therein). The uncertainties can be minimized through ambient measurements at regional and local scales, thereby assessing the effectiveness of the MP and relevant national regulations on spatial scales that cannot be inferred from globally averaged remote location data. In addition, such ambient measurements can serve as the first step in developing top-down emission estimates using inversion algorithms coupled with atmospheric dispersion models (Hurst et al., 2006; Stohl et al., 2009; Keller et al., 2012). These regional-scale estimates can consequently provide a unique and independent tool to evaluate official emission inventories (Keller et al., 2012).

To date, atmospheric halocarbons in Asia have mainly been measured in East Asia, especially Japan and the Pearl River Delta (PRD), China (Palmer et al., 2003; Yokouchi et al., 2005a; Chan and Chu, 2007; Guo et al., 2009; Vollmer et al., 2009; Stohl et al., 2010; Zhang et al., 2010, 2014; Shao et al., 2011; Li et al., 2014; Wu et al., 2014). A fraction of these studies reported top-down halocarbon emission estimates using inverse modelling (Vollmer et al., 2009; Stohl et al., 2010), the CO tracer method (Palmer et al., 2003; Guo et al., 2009; Shao et al., 2011; Fang et al., 2012; Zhang et al., 2014) or the HCFC-22 tracer method (Fang et al., 2012; Wu et al., 2014). Aircraft-based measurement campaigns have been conducted in the region centering over the Indonesian archipelago (BIBLE A; Elliott et al., 2003), Java (BIBLE B; Choi et al., 2003), the northwestern and western Pacific basin extending near Borneo (NASA PEM-West A and B; Blake D.R. et al., 1996, 1997), Thailand and Malaysia (CARIBIC, Leedham Elvidge et al., 2015). In comparison, relevant measurements focusing exclusively on Southeast (SE) Asia are almost nonexistent except for an early ship-based report on marine-derived halocarbons (Yokouchi et al., 1997) and a more recent land-based study of 4 short-lived halocarbons from the Malaysian Borneo (Robinson et al., 2014).

To enhance our understanding of halocarbon levels in SE Asia, two ground-based measurement campaigns were conducted in 2011–2012 in Singapore, an urban-industrial city-state characterized by a warm and humid tropical environment. This work was part of the 7 Southeast Asian Studies (7SEAS) campaign investigating burning smoke of peat-forest and agricultural residue in the Maritime Continent. Another major objective of the study was to investigate the effects of industrial emissions on halocarbon levels. Singapore is a major center for chemical, petrochemical, pharmaceutical, electronics and other manufacturing industries that are clustered in industrial areas/estates across the mainland as well as on nearby islands. In addition, the close proximity to industrial areas in neighboring countries (e.g., Malaysia (N and NE of Singapore) and Indonesia (W-SW of Singapore)) implies possible mixing of regional emission plumes with local ones and could potentially affect observed halocarbon levels.

This work quantified a total of 26 atmospheric halocarbons – one of the largest suites reported in the past ~10 years and higher than the 9 to 16 halocarbon species typically characterized by studies across the world (Reimann et al., 2008; Keller et al., 2012; Artuso et al., 2010). A list of halocarbons measured in this study along with their major uses/sources, atmospheric lifetimes, ODPs, 100-y global warming potentials (GWPs) and applicable phase-out timelines are provided in Table S1 (Supplementary material). The halocarbon dataset is supplemented by measurements of 7 non-methane hydrocarbons (NMHCs; ethane, ethyne, propane, i-butane, n-butane, benzene and toluene), 7 alkyl nitrates (C_1-C_5 $RONO_2$), 2 sulfur gases (carbonyl sulfide and dimethyl sulfide; OCS and DMS), and carbon monoxide (CO) to better understand sources and atmospheric processes. These observations enable an evidence-based assessment of – i) the effectiveness of MP and related national regulations on ODS levels; ii) the influence of the growth in use of first- and second-generation CFC replacements; and iii) the relative impacts of

natural and anthropogenic sources on short-lived halocarbons. Discussion is also provided on quantitative source contributions determined from the receptor model positive matrix factorization (PMF) in terms of their significance, regional effects and local emissions.

2. Materials and methods

2.1. Study location and canister sampling

Singapore (1°17′ N, 103°50′E) is an urbanized and industrialized city-state in SE Asia with a land area of 719.1 km^2 and a population density of 7737 people km^{-2} (http://data.worldbank.org/indicator/EN.POP.DNST). Situated at ~15 m above the mean sea level, the city experiences tropical climate, with relatively uniform temperatures of 25°–32 °C, high relative humidity (RH, 61 − 90%) and abundant rainfall (~2300 mm yr^{-1}) (Department of Statistics, 2016). Seasonality in Singapore comprises of two monsoons coupled with two inter-monsoon periods; the northeast (NE) monsoon generally ranging from November to March, and the southwest (SW) monsoon from June to September (Department of Statistics, 2016).

Whole air samples were collected in 2-L electropolished, conditioned stainless steel canisters that were cleaned and conditioned at the University of California Irvine (UC Irvine) laboratory using a repeated pump-and-flush method followed by evacuation. Briefly, prior to shipment to the field, each canister was taken to the UC Crooked Creek Station research facility in the Sierra Nevada Mountains (altitude = 10,200 ft) where it was pressurized with ambient air (to 40 psig for 2 min) and then flushed to ambient pressure. This pump-and-flush step was repeated three times before the cans were returned to the UC Irvine laboratory, where they were flushed with ultra-high purity He and evacuated to 10^{-2} Torr using a pump-out manifold (E2M12 dual-stage vacuum pumps, Edwards Vacuum, Wilmington, MA). The He pump-and-flush procedure was also repeated three times, before a final evacuation to 10^{-2} Torr. Lastly each canister was humidified by adding ~17 Torr of purified water (the approximate vapour pressure of water at room temperature) in order to minimize surface adsorption and to improve the reproducibility of analytical split ratios during laboratory analysis.

Sampling was carried out on the rooftop of Engineering Block E2 (1°18′N, 103°46′E, 67 m above mean sea level) at the National University of Singapore during August to October of 2011 and 2012. Specifically, samples were collected during 18th August–31st October 2011 and 16th August–1st November 2012. An on-site meteorological station measured temperature, RH, solar insolation, rainfall, wind speed and wind direction every 5 min (https://inetapps.nus.edu.sg/fas/geog/). A detailed map of the study area showing location of the receptor sampling site in Singapore is presented in Fig. 1. Throughout the study period, air masses representing various sectors of the city as well as neighboring regions were sampled (see Section 3.4 and Fig. 5 for details). A total of 166 whole air samples were collected in Singapore with 71 and 95 samples collected in 2011 and 2012, respectively. One sample per day was collected on 44 occasions while for the rest of the period, 2 samples were collected per day, typically one in the morning (9–11 AM) and one in the afternoon (3–5 PM). Overall, around 33% of the samples were collected in the morning while the remaining ~67% were collected in the afternoon. Only 8 out of the 166 samples were collected at nighttime (after 6 PM). A total of 23 out of the 166 samples collected at the receptor site were affected by transboundary peat-forest smoke. These 23 samples were classified as smoke-dominant while the rest (n = 143) were categorized as non-smoke dominant. Sample categories were determined by adopting HYSPLIT air-parcel backward trajectories (http://ready.arl.noaa.gov/HYSPLIT.php), hotspot maps of the Maritime Continent (https://www.nrlmry.navy.mil/aerosol_web/7seas/7seas.html), weather conditions, and concentrations of aerosol organic markers of biomass burning (levoglucosan and malic acid). The criteria and effects of sample classification are detailed in a separated article (Lan et al., 2017, Manuscript in preparation). In addition to receptor samples, 8 canister samples were collected near burning sites in southern Riau, Indonesia (0°17′S, 102°25′E, 701 m above mean sea level, Fig. 1) on 3 December 2011 to study effects of peat-forest fires on the levels of specific halocarbons and to compare with receptor data. All canisters containing sampled air were shipped to and analyzed in the laboratory at UC Irvine.

2.2. Analysis of halocarbons and other VOCs

Each whole air sample was analyzed for >100 VOCs at the UC Irvine laboratory, and a subset of the VOC suite is presented in this work. The samples were analyzed using three gas chromatographs (GCs) coupled with a suite of detectors that together are sensitive to the range of target VOCs. Flame ionization detectors (FIDs) were used to measure C_2-C_{10} hydrocarbons, electron capture detectors (ECDs) for C_1-C_2 halocarbons and C_1-C_5 alkyl nitrates, and a quadrupole mass spectrometer detector (MSD) for unambiguous compound identification and selected ion monitoring. For each sample a 1520 cm^3 sample aliquot was introduced into the analytical system's manifold and passed over glass beads contained in a loop maintained at liquid N_2 temperature. The flow was regulated by a Brooks Instrument mass flow controller (model 5850E) and was kept below 500 cm^3 min^{-1} to ensure complete trapping of the target compounds (e.g., halocarbons, hydrocarbons) while allowing more volatile components (e.g., N_2, O_2, Ar) to be pumped away. The target compounds were re-volatilized by immersing the loop in hot water (80 °C), and were then flushed into a He carrier flow (head pressure 48 psi). The sample flow was then split into five streams, which were

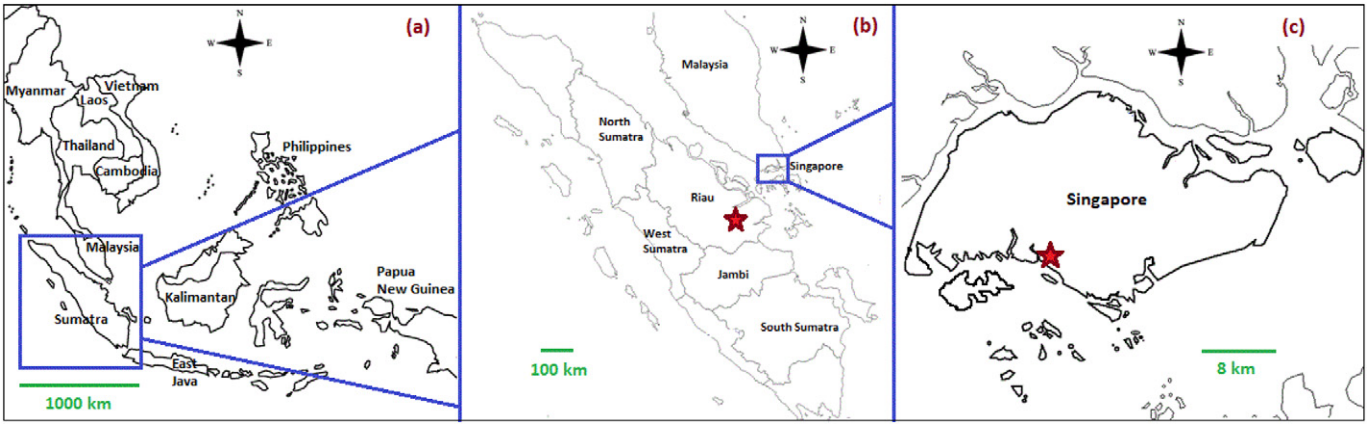

Fig. 1. Map of Southeast Asia (a) showing locations of the sampling sites (red stars) in Riau, Indonesia for near-source samples (b) and NUS, Singapore for receptor samples (c).

chromatographically separated on an individual column and sensed by a single detector: (1) FID with DB-1 column (60 m, I.D. 0.32 mm, film thickness 1 μm); (2) FID with Na_2SO_4 PLOT (30 m, I.D. 0.53 mm, film thickness 10 μm) + DB-1 (5 m, I.D. 0.53 mm, film thickness 1 μm) columns; (3) ECD with Restek 1701 column (60 m, I.D. 0.25 mm, film thickness 0.5 μm); (4) ECD with DB-5 (30 m, I.D. 0.25 mm, film thickness 1 μm) + Restek 1701 (5 m, I.D. 0.25 mm, film thickness 0.5 μm) columns; (5) MSD with DB-5MS column (60 m, I.D. 0.25 mm, film thickness 0.5 μm).

Zero-air and N_2 for use in the FIDs and ECDs were generated in-house. House air was passed through an aqua pure water filter (CUNO Inc., AP101T) filled with glass wool, then through an air dryer (Whatman, 64-02) equipped with a 100-12 BX pre-filter. This removed oil, water, and particulates from the air stream, which was then split and directed into a nitrox-N_2 generator (Domnick Hunter, NG7-0) and a zero-air generator (Praxair, Airlab WHA 76803). Before entering the analytical system, all gases were passed through homemade graphite/molecular sieve traps to remove any remaining contaminants. Both FIDs operated at a detector temperature of 250 °C with a zero-air flow of 450 mL min^{-1}, an H_2 flow of 40 mL min^{-1} and a detector makeup gas flow of 20 mL min^{-1} N_2. The ECDs operated at a detector temperature of 250 °C with a detector makeup flow of 50 mL min^{-1} N_2.

Quality assurance-quality control (QA-QC) parameters for halocarbon and other VOC measurements are presented in Table S2 (Supplementary material). Limits of detection (LOD) varied from 0.01 pptv for the halomethanes to 10 pptv for CFC-12 while analytical precision ranged from <1% for CFC-11 and CFC-12 to 7–9% for dibromochloromethane and bromochloromethane. Analytical accuracy was highest for CFCs at 2–5% followed by halons, CCl_4, CH_3CCl_3, HCFC-22, $CHCl_3$, C_2HCl_3, CH_3Br and CH_3I at ~5%, and the rest at 10–20%. For other VOCs, the LOD ranged from 0.02 pptv for $RONO_2$ to 10 pptv for OCS and DMS. Analytical precision and accuracy ranged from 0.5–3% and 5–10%, respectively.

2.3. Source apportionment

Potential sources of halocarbons were apportioned using positive matrix factorization (PMF5.0; US EPA, 2014). A total of 166 samples and 37 species (including the sum of all input gases i.e., total gases, TG) were used. These included 19 halocarbons, 2 sulfur gases (OCS and DMS), 7 NMHCs (ethane, ethyne, propane, i-butane, n-butane, benzene and toluene), 7 alkyl nitrates, and CO in addition to TG. Out of the 26 quantified halocarbons, 19 were selected as inputs for PMF based on their applicability as source markers. Measurement data for H-2402, CFC-114 and HFC-152a in this study were available only for 2012 while that for H-1301 were available only for 2011. Consequently, these species were excluded from PMF because of the substantial number of missing values. Details of input data pre-treatment (including calculation of enhancements), PMF model runs, factor selection, goodness of fit results and error estimation are provided in the Supplementary material.

3. Results and discussion

Based on their ODP, GWP and atmospheric abundance, Table 1 lists the mixing ratios of the 21 most important halocarbons measured in Singapore, and at other locations throughout the world. Data for 5 other halocarbons, NMHCs, $RONO_2$, OCS, DMS and CO are provided in the Supplementary material (Table S3). Table 1 also provides atmospheric enhancements of the 21 selected halocarbons relative to global tropospheric backgrounds. In this work, median mixing ratios of individual compounds are used to discuss observed levels and to calculate enhancements. This is used as a conservative approach in order to minimize a biased assessment since mean mixing ratios can be substantially influenced by outliers. For example, the mean mixing ratio of C_2Cl_4 (53 ± 286 pptv) is ~59 times the tropospheric background (Table 1), owing mainly to the presence of outliers, especially two extreme values of 982 and 3533 pptv. The enhancement is reduced drastically to a factor of 6.6 if the median concentration (6 pptv) is chosen over the mean thus down-weighting the influence of outliers.

3.1. Effects of Montreal Protocol (MP) and related regulations on halocarbon levels

Measured median mixing ratios of ODS such as CFCs, halons, CCl_4 and CH_3CCl_3 in Singapore show enhancements of 1–17% over global tropospheric background levels, comparable to enhancements observed at the two remote locations listed in Table 1, which deviate from the global background by 2–12% (except CH_3CCl_3). These values are in sharp contrast to those for first- and second-generation CFC replacements that typically show enhancements of orders of magnitude over baseline (see Section 3.2). This indicates that the measured mixing ratios of CFCs, halons, CCl_4 and CH_3CCl_3 are residuals from operations phased out after the implementation of MP rather than emissions from presently active sources. Despite being an Article 5 signatory to the MP and thus being allowed a longer timeframe (until 2010) for phase-out, Singapore implemented prohibitions on the import and use of ODS during 1992–1996, well ahead of schedule (NEA, 2016). Our measurements conducted ~20 years after this phase-out provide the first evidence of the effectiveness of MP regulations on atmospheric levels of ODS in Singapore.

In the pre-MP era, CFCs (CFC-11, CFC-12, CFC-113 and CFC-114) were used as refrigerants, aerosol spray propellants and closed cell foam blowing agents (Chan and Chu, 2007). Singapore instituted a ban on the import of CFCs in 1996; consequently, current enhancements of CFCs observed here are only 3–9% over background. The temporal trends of CFCs (Fig. 2a) with small overall relative standard deviations (RSDs) of <5% also suggest stabilized levels. A comparison of measured CFC enhancements in Singapore with those from other parts of the world (Table 1) and long-term trends therein reveals that reduction rates after the MP implementation vary considerably, depending on the phase-out timeline and the extent of regional industrialization. For example, remote locations in Europe and the Mediterranean exhibit a steady decline of 1–2 ppt y^{-1} for CFCs in the decades after the implementation of the MP regulations (Reimann et al., 2008; Artuso et al., 2010). In comparison, studies from PRD and Hong Kong report a much smaller rate of decline (0.008–0.17 ppt y^{-1}) and higher mixing ratios of CFCs relative to Singapore (Chan and Chu, 2007; Zhang et al., 2010). This is likely a result of the high density and rapid growth of the industrial agglomeration in this region coupled with the later start date to phase-out CFCs in China around 2000 (Zhang et al., 2010). Despite the dramatic fall in CFC production and emission across the world in the post-MP era, a significant CFC bank, projected at 8302 $MtCO_2$-eq in 2015, is still in existence and contributes to regional backgrounds through leakage (IPCC/TEAP, 2005; Kim et al., 2011).

The median halon levels measured in Singapore during this study have stabilized and are similar to tropospheric background levels with enhancements of 0.3%, 11% and 17% for H-1301, H-1211 and H-2402, respectively. These enhancements are comparable to those reported from remote locations (Table 1). The temporal trend of H-2402 shows a homogenous distribution (RSD: 3%) while H-1211 and H-1301 are characterized by transient peaks (Fig. 2a), possibly related to leakage from fixed and/or portable fire protection units in the nearby areas. Halons were widely used as fire extinguishing agents and, to a lesser extent, in refrigeration (Chan and Chu, 2007; Zhang et al., 2010) before the MP regulations were implemented. Singapore prohibited the use of H-1301 for new fire protection systems in 1992, and the import of H-1301, H-1211 and fire extinguishers filled with H-1211 in 1994. The import of H-2402 was banned in 1992. Consequently, the small enhancements observed here suggest residual levels rather than inputs from continued use. Recent studies have reported either small increases (0.03–0.09 ppt y^{-1}) (IPCC/TEAP, 2005; Reimann et al., 2008) or short-term reductions (Artuso et al., 2010) of global long-term halon trends. Between 2010 and 2014, global H-1211 levels decreased by 0.09 ppt y^{-1} while H-

Table 1
Mixing ratios (pptv) of selected halocarbons in Singapore (2011—2012), global tropospheric backgrounds[a] and at other locations across the world. Halocarbons are listed in an increasing order of their median enhancements above global tropospheric backgrounds.

Species	Singapore			Global background[a]	Mean enhancement	Median enhancement	PRD, China[b]	Hong Kong, China[c]	Bristol, UK[d]	K-Puszta, Hungary[e]	Lampedusa Island, Mediterranean Sea[f]	Jungfraujoch, Switzerland[g]
	Mean ± 1σ (RSD) (pptv)	Median (pptv)	Range (pptv)	(pptv)	(%)	(%)	(Industrial) (pptv)	(Urban) (pptv)	(Urban) (pptv)	(Remote) (pptv)	(Remote) (pptv)	(High-alpine) (pptv)
H-1301	3.8 ± 1.9 (51%)	3.31	3.0–18.3	3.3	15	0.3					3 ± 0.1	3 ± 0.2
CFC-12	541.5 ± 20.9 (4%)	534.0	520.0–649.0	528.3	3	1	578	615 ± 17	545 ± 46	542 ± 3		545 ± 2
CFC-11	248.9 ± 10.8 (4%)	247.0	232.0–292.0	236.0	6	5	274	294 ± 7	263 ± 73	253 ± 2		248 ± 1
HCFC-142b	23.7 ± 3.6 (15%)	22.9	20.1–45.1	21.8	9	5	17	32 ± 16		22 ± 0.4	19 ± 0.4	19 ± 0.4
CFC-113	79.1 ± 3.3 (4%)	78.4	72.9–90.5	74.2	7	6	163	96 ± 6			76 ± 1	77 ± 0.2
CFC-114[h]	17.9 ± 1.0 (5%)	17.7	16.2–20.1	16.3	9	9	15					17 ± 0.1
CCl_4	93.5 ± 5.7 (6%)	92.5	86.7–130.9	84.4	11	10	107	121 ± 4	92 ± 33		90 ± 2	88 ± 1
CH_3CCl_3	6.3 ± 0.8 (12%)	6.1	5.2–9.5	5.5	14	10	69		25 ± 11		12 ± 0.4	15 ± 0.1
H-1211	5.5 ± 3.6 (65%)	4.5	4.0–36.8	4.0	36	11	18			5 ± 0.4	4 ± 0.2	5 ± 0.1
H-2402[h,i]	0.53 ± 0.02 (3%)	0.53	0.51–0.64	0.45	18	17	0.49					
HCFC-141b	52.9 ± 60.0 (113%)	30.8	19.5–377.1	22.1	140	39	18	56 ± 13		23 ± 0.6	21 ± 0.5	21 ± 0.1
HCFC-22	510.9 ± 534.0 (105%)	356.5	214.0–5021.0	217.1	135	64	214	322 ± 41	315 ± 483	214 ± 4	205 ± 4	195 ± 1
HFC-152a[h]	46.7 ± 114.8 (246%)	11.1	7.0–730.8	6.7	597	65				10 ± 1		7 ± 0.2
HFC-134a	187.1 ± 403.0 (215%)	111.0	60.4–4898.4	66.5	181	67	19			73 ± 17	58 ± 1	46 ± 0.3
CH_3Cl	976.7 ± 277.6 (28%)	896.5	630.0–2611.0	523.7	86	71	701		534 ± 181		551 ± 12	
$CHCl_3$	33.4 ± 40.7 (122%)	18.0	8.8–242.0	7.6	340	137	31	43 ± 7	39 ± 56		11 ± 0.3	
CH_3I[j]	6.2 ± 18.9 (303%)	1.2	0.29–140.7	0.5	1148	147					0.7 ± 0.1	
CH_3Br	31.4 ± 36.7 (117%)	21.4	8.0–333.2	7.0	346	204	13	19 ± 4	16 ± 8		9 ± 0.3	
CH_2Cl_2	343.7 ± 761.7 (222%)	90.4	12.2–5744.7	21.7	1484	316	561	948 ± 306	289 ± 387		48 ± 2	
C_2Cl_4	53.0 ± 285.6 (539%)	5.6	1.0–3532.9	0.9	5721	520	50	167 ± 47	35 ± 59			
C_2HCl_3	16.8 ± 29.8 (178%)	5.6	0.1–230.2	0.06	27,835	9292	38	465 ± 179	34 ± 93			

Note: number of samples = 71 for H-1301, 92 for HFC-152a, 95 each for CFC-114 and H-2402 and 166 each for the rest. Enhancements of mean and median halocarbon mixing ratios in Singapore (expressed as %) are calculated relative to the global tropospheric background.

[a] Global tropospheric background calculated from AGAGE global mean data for each species during Aug–Oct 2011 and Aug–Oct 2012.
[b] Median mixing ratios at Pearl River Delta (PRD) in China, Chan and Chu (2007).
[c] Guo et al. (2009), mean ± 1σ.
[d] Khan et al. (2009), mean ± 1σ.
[e] Keller et al. (2012), mean ± 1σ.
[f] Artuso et al. (2010), errors represent measurement uncertainties.
[g] Reimann et al. (2008), errors represent measurement uncertainties.
[h] During Aug–Oct 2012.
[i] Background for H2402 calculated from NOAA ESRL data for Barrow, Alaska during Aug–Oct 2012.
[j] Background for CH_3I calculated from Alert, Canada data for 2011 (Yokouchi et al., 2012).

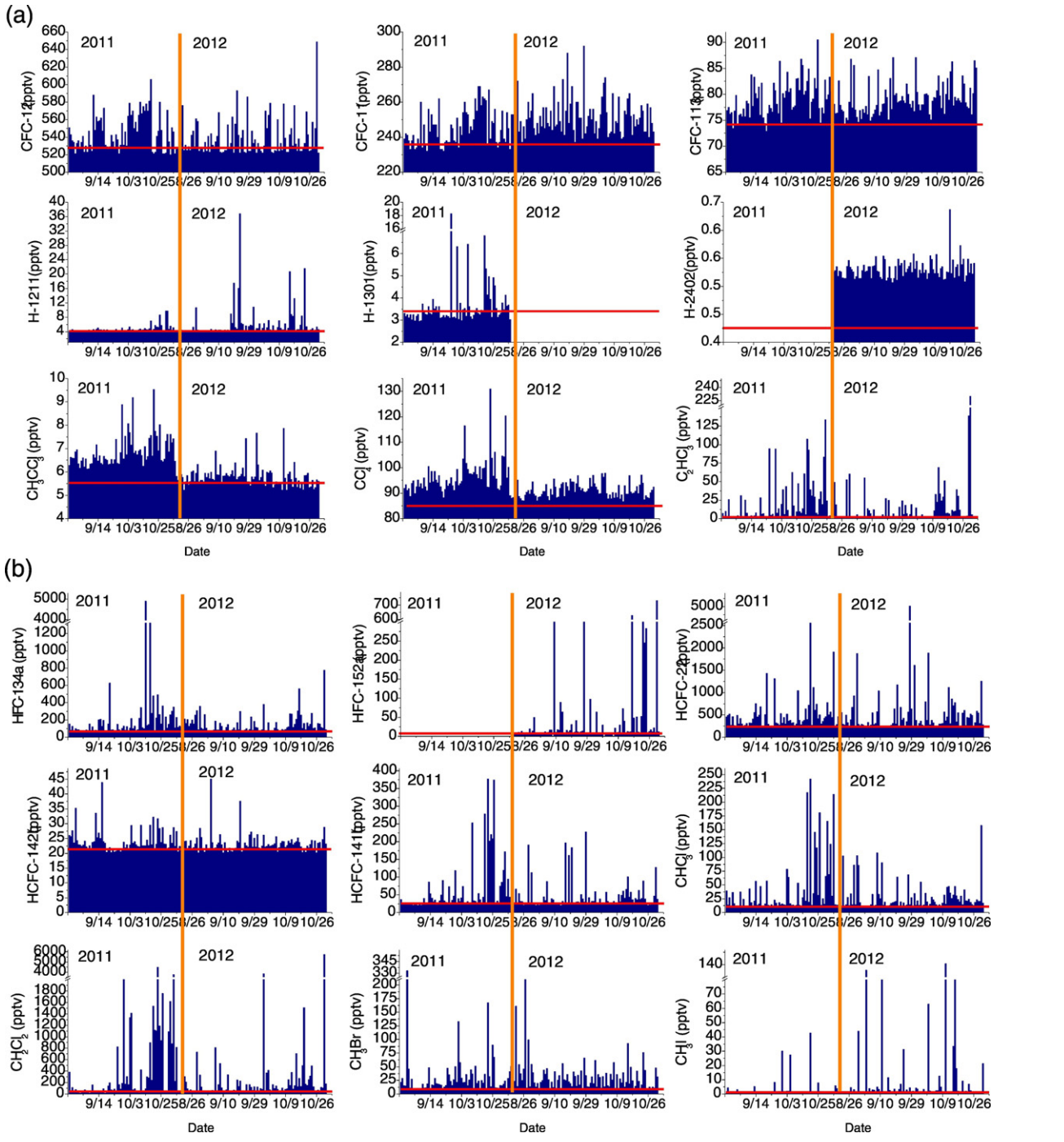

Fig. 2. Time-series of selected halocarbons for the study period (Aug–Oct 2011–2012). The sub-plots show individual time series for CFCs, halons, CCl_4, CH_3CCl_3 and C_2HCl_3 (sub-plot: a), and those for HCFCs, HFCs, $CHCl_3$, CH_2Cl_2, CH_3Br and CH_3I (sub-plot: b). Orange vertical lines separate samples collected during 2011 and 2012 while red horizontal lines represent global tropospheric background values for individual species. Note that sampling was not continuous during the study period and measurement gaps between individual samples are not shown.

1301 exhibited small increases of 0.02–0.03 ppt y^{-1} (Prinn et al., 2016; ESRL, 2016). Similar to CFCs, a halon bank (consisting of H-1301 and H-1211), projected at 206 $MtCO_2$-eq in 2015, also still exists and contributes to atmospheric levels via leakage (IPCC/TEAP, 2005; Kim et al., 2011). It is estimated that leakage from the halon bank amounts to 2 ± 1% y^{-1} and 4 ± 2% y^{-1} for fixed and portable fire protection systems, respectively (IPCC/TEAP, 2005).

Among other ODS reported in this study, median levels of CCl_4 and CH_3CCl_3 are enhanced by ~10% above background levels (Table 1) and exhibit relatively stable temporal distributions (RSDs: 6–12%, Fig. 2a). CH_3CCl_3 and CCl_4 were employed extensively as solvents in commercial and industrial applications (Artuso et al., 2010) before their import into Singapore was banned in 1996 under MP regulations. Measured levels of CCl_4 and CH_3CCl_3 in Singapore are lower by 20–30% and ~90%, respectively, compared to other urban-industrial centers in Asia (Table 1), showing the effectiveness of this early phase-out. In terms of long-term trends from other sites across the world, steady reductions of CH_3CCl_3 and CCl_4 levels in the order of 1–3.5 ppt y^{-1} and 0.1–0.3 ppt y^{-1} have been reported from a remote site in Europe (Reimann et al., 2008) and an urban location in Hong Kong (Zhang et al., 2010), respectively.

Despite scattered reports of unexpected increasing trends in CCl_4 from PRD (0.002 ppt y^{-1}) (Zhang et al., 2010) and the remote Mediterranean (5.7 ppt y^{-1}) (Artuso et al., 2010), the overall global trend of CCl_4 in recent years is one of gradual reduction (Prinn et al., 2016; ESRL, 2016). It is noted though that the rates of reduction of CCl_4 observed across the world are far lower than expected given its atmospheric lifetime and the absence of continued emission inputs. Using inverse modelling, Hu et al. (2016) have recently reported an average US emission of 4 Gg y^{-1} during 2008–2012 from non-dispersive uses of CCl_4 and observed that this value is 2 orders of magnitude higher than the reported inventory. An emission of 2.2 Gg y^{-1} from Europe during 2006–2014, mainly from chlor-alkali plants, has been reported by Graziosi et al. (2016). A combined regional top-down emission estimate of 21 Gg y^{-1} has been proposed for US, Europe, China and Australia (SPARC, 2016). In contrast, bottom-up inventories including feedstock and process agent uses, by-product emissions from chloromethanes and perchloroethylene plants, and legacy emissions are estimated to account for ~25 Gg y^{-1} (SPARC, 2016). These emissions do not close the global CCl_4 discrepancy of 54 Gg y^{-1} (WMO, 2014), and indicate an underestimation of the total CCl_4 lifetime in the environment. Using updated values of ocean and soil lifetimes of CCl_4, a revised total lifetime of 32–33 y has recently been proposed (Butler et al., 2016; SPARC, 2016) that has substantially narrowed the observed CCl_4 discrepancy.

3.2. CFC replacements (HCFCs and HFCs) and relevant regulation

Among first-generation CFC replacements, HCFC-22 and HCFC-141b dominate the total HCFC profile observed in Singapore (Table 1, Fig. 2b), with median mixing ratios that are 64% and 39% higher than background levels, respectively. HCFC-22 levels in Singapore are higher by 11–67% as compared to the PRD and Hong Kong (Table 1). The main use of HCFC-22 is as an alternative to CFC-11 and CFC-12 in the manufacturing of refrigerants and propellants, while HCFC-141b is used mainly as a foam blowing agent and refrigerant (Chan and Chu, 2007; Artuso et al., 2010). Following the CFC phase-out, production of these first-generation interim substitutes increased substantially with their annual global production peaking in the late 1990s (AFEAS, 2006; Kim et al., 2011). Although the production and consumption of HCFCs declined in developed countries since the early 2000s, those for Article 5 countries increased dramatically with HCFC-22 comprising ~77% of the total HCFC budget until 2006 (Kim et al., 2011). As a result, HCFC-22 levels in remote locations in the Mediterranean and Europe have shown increases of 6.2 ppt y^{-1} (2005–2008) and 4.3 ppt y^{-1} (2004–2006), respectively (Reimann et al., 2008; Artuso et al., 2010), while inland PRD and Hong Kong have recorded lower but steady growths (1.2 and 2.4 ppt y^{-1}, respectively) (2001–2007) (Zhang et al., 2010).

The low observed abundance, on the other hand, of HCFC-142b over baseline (5%) in this study indicates the presence of a regional background rather than active use. In addition to Singapore, halocarbon consumption in neighboring countries (i.e., Malaysia and Indonesia) could potentially contribute to the observed level; however, consumption of HCFC-142b in these countries is negligible compared to other HCFC variants. For example, 2009 consumption of HCFC-142b in Malaysia was only 4.2 MT as compared to 1335 MT of HCFC-141b and 7700 MT of all HCFC variants combined (UNDP, 2012). Indonesia did not consume HCFC-142b in 2009, while figures for HCFC-141b and total HCFC consumption were 1186 and 5832 MT, respectively (UNEP, 2011).

Among second-generation CFC replacements (i.e., HFCs), HFC-134a and HFC-152a are widely used for refrigeration and mobile air conditioning (O'Doherty et al., 2004), which explains the observed enhancements of 67% and 65%, respectively (Table 1). The median HFC-134a mixing ratio observed in this study is higher by 1.5–2 times over remote locations whereas that for HFC-152a is higher by factors of 1.1–1.6 (Table 1). HFCs were introduced as alternative refrigerants in the 1990s with the production of HFC-134a peaking at ~2005 and those of HFC-152a and HFC-125a increasing steadily during 2003–2007 (Kim et al., 2011). Consequently, IPCC/TEAP (2005) reported that tropospheric concentrations of individual HFCs increased by 0.3–4 ppt y^{-1} between 2001 and 2003, based on data from global monitoring networks. High annual rates of increase (4.7–4.8 ppt y^{-1}) in atmospheric HFC-134a levels have also been reported from European high-alpine and remote Mediterranean locations during 2004–2008 (Reimann et al., 2008; Artuso et al., 2010).

It follows from the discussion so far that in the post-MP era, these first- and second-generation CFC replacements have emerged as the dominant halocarbon species in Singapore. Given the large GWPs of HCFC-22, HFC-134a and HCFC-141b of 1810, 1430 and 725, respectively, their increasing atmospheric abundances are of concern. These environmental concerns have been addressed in a timely manner under the newly-instituted HCFC phase-out management plans (HPMPs) in Singapore and other SE Asian countries with sharp declines projected for the region in the near future. As part of the MP regulations, Singapore instituted an HPMP in 2013, capping the quantity of HCFC at 216 ODP tons (mean of 2009 and 2010) with planned reductions of 10% by 2015, 35% by 2020, 67.5% by 2025 and 97.5% during 2030–2040 (NEA, 2012). Between 2011 and 2014, HCFC consumption in Singapore declined substantially as compared to 2009–2010 values and averaged 126 ± 28 ODP tons (range: 110–169 ODP tons) (http://ozone.unep.org/reporting/). Other regional consumers, Indonesia and Malaysia, have also developed and started implementation of corresponding HPMPs from 2012, with substantial emission reductions starting in 2016 (UNEP, 2011; UNDP, 2012). Larger consumers in Asia (India and China) have similarly capped HCFC production and consumption between 2013 and 2016 with 100% phase-out targeted during 2030–2040. While regional HCFC levels in SE Asia might show faster declines resulting from relatively lower consumption rates in Malaysia, Indonesia and Singapore, global HCFC levels are likely to be constrained mostly by emissions from larger consumers such as China, USA, South Korea and India, with HCFC-22 consumptions of 18,603, 3396, 1769 and 1599 ODP tons, respectively, in 2009 (Saikawa et al., 2012). Despite efforts at an accelerated phase-out, NOAA has estimated that global atmospheric abundances of HCFCs will increase in the next two decades, reflecting increasing consumption, and will reach peak values around 2030 followed by a decline (WMO, 2010). This projection is contested by other studies that estimate, for example, that HCFC-22 emissions from China will peak at 134 Gg y^{-1} in 2016 followed by a steady decline to 10 Gg y^{-1} in 2050 under the MP-related phase-out scenario (Li et al., 2016).

3.3. Short-lived halocarbons (SLHs)

An important subset of halocarbons is represented by short-lived species such as methyl halides (CH_3Cl, CH_3Br and CH_3I), trichloromethane and tribromomethane ($CHCl_3$ and $CHBr_3$), dichloromethane and dibromomethane (CH_2Cl_2 and CH_2Br_2), tetrachloroethylene (C_2Cl_4), and trichloroethylene (C_2HCl_3) with atmospheric lifetimes in the order of weeks to about a year (Table S1, Supplementary material). Their environmental importance stems from their ability to contribute to stratospheric O_3 loss by acting as Cl, Br and I carriers (Kurylo et al., 1999; Artuso et al., 2010). Unlike CFCs, halons, HCFCs and HFCs, which are sourced exclusively from industrial operations, these short-lived species are known to have a multitude of sources, both natural and anthropogenic. In this section, levels and potential sources of these SLHs are discussed by employing photochemical ages of air masses, clustered trajectory analyses, halocarbon ratios, and corresponding associations. A number of NMHCs, C_1-C_5 alkyl nitrates, DMS and CO are used to aid the investigation.

3.3.1. Photochemical ages of air masses

First, the extent of photochemical processing of air masses sampled at the receptor site is estimated by comparing observed ratios of individual alkyl nitrates ($RONO_2$) to their parent hydrocarbons (RH) to values

predicted using a simplified sequential reaction scheme (Bertman et al., 1995; Simpson et al., 2003; Zhou et al., 2005; Russo et al., 2010; Swarthout et al., 2013).

$$\frac{[RONO_2]}{[RH]} = \frac{k_A}{(k_B - k_A)}\left(1 - e^{(k_A - k_B)t}\right)$$

Here, k_A and k_B are pseudo-first order rate constants for the sequential production and destruction, respectively, of $RONO_2$ and the factor β takes into account branching ratios that lead to $RONO_2$ formation, assuming no peroxy radical self-reaction (Simpson et al., 2003). The equation above assumes a zero initial concentration of $RONO_2$. Values of k_A, k_B and β are taken from Simpson et al. (2003), and predicted and observed $[RONO_2]/[RH]$ ratios for C_2-C_5 $RONO_2$ are plotted against 2-butyl nitrate to n-butane ($[2\text{-}BuONO_2/\text{n-butane}]$) in Fig. 3. The selected C_2-C_5 $RONO_2$ are ethyl nitrate ($EtONO_2$), 1- and 2-propyl nitrates (1-$PrONO_2$ and 2-$PrONO_2$, respectively), and 2- and 3-pentyl nitrates (2-$PeONO_2$ and 3-$PeONO_2$, respectively). The choice of $[2\text{-}BuONO_2/\text{n-butane}]$ as the x-axis in Fig. 3 is based on the large abundances of 2-$BuONO_2$ and the precursor n-butane (median: 10 and 1495 pptv, respectively) in this study and the fact that 2-$BuONO_2$ does not have other significant formation pathways (Roberts et al., 1998).

Three major observations are noted from Fig. 3, which are – i) most of the samples at the receptor exhibit photochemical aging of less than a day, with the largest fraction showing ages of 6 h to 1 day, indicating the relatively young nature of air masses. This signifies that $RONO_2$ precursors were emitted either locally in Singapore or from neighboring countries in the close vicinity; ii) no systematic difference in photochemical ages is observed between peat-forest smoke dominated and non-smoke dominated samples at the receptor. In terms of C_2-C_5 $RONO_2$ mixing ratios, the smoke-dominated samples are enriched by 17–34% (median values) over the non-smoke category, suggesting enhanced release of alkane precursors from peat fires; iii) the $[EtONO_2/\text{ethane}]$ ratios (Fig. 3a) lie significantly above the pure photochemistry curve, especially for short processing times. Similar observations have been reported previously by a number of authors (Bertman et al., 1995; Simpson et al.,

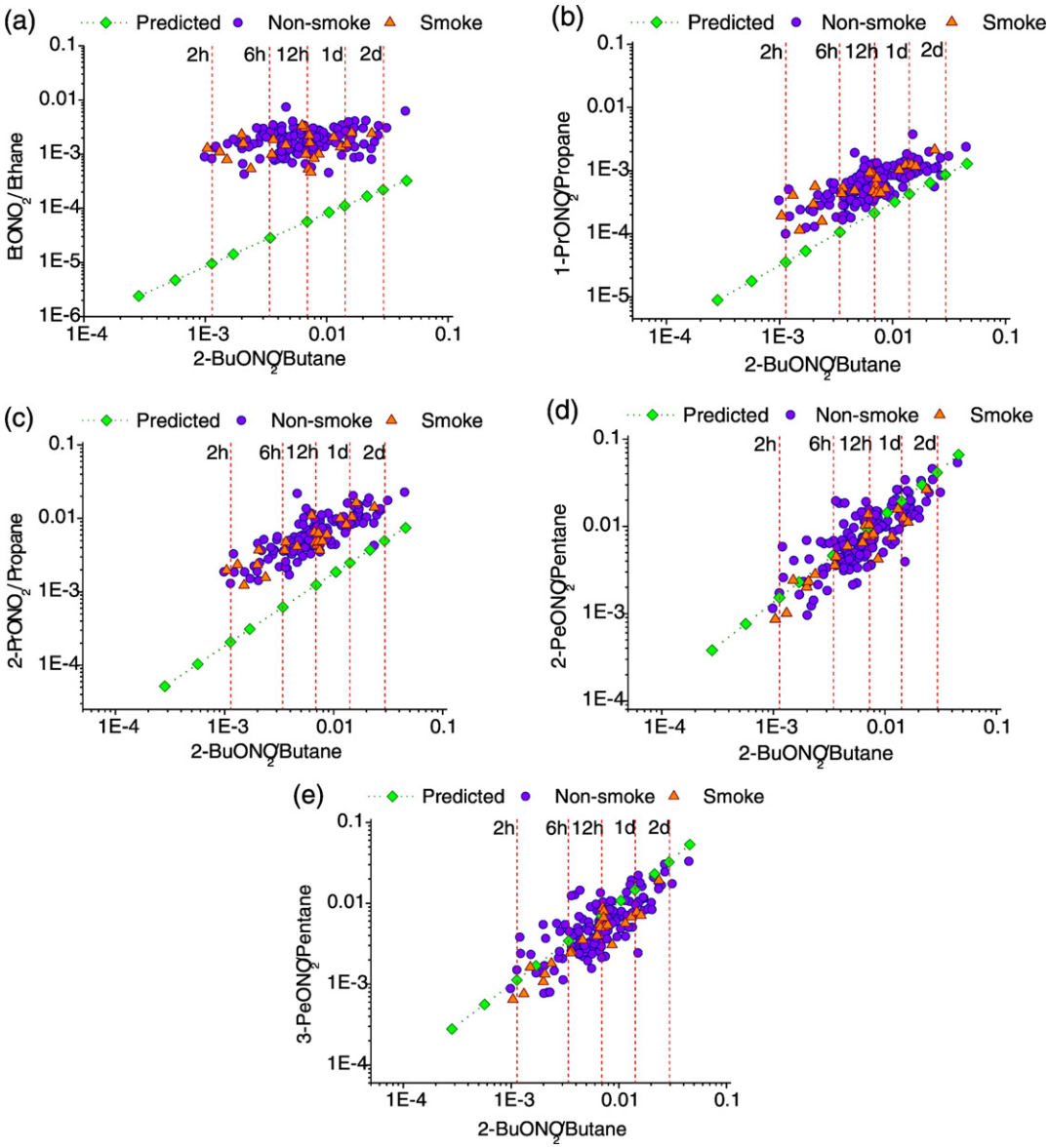

Fig. 3. Photochemical ages of C_2-C_5 alkyl nitrates for receptor samples collected in Singapore. Sub-plots show relationships between 2-$BuoNO_2$/Butane and $EtONO_2$/Ethane (a), 1-$ProNO_2$/Propane (b), 2-$ProNO_2$/Propane (c), 2-$PeONO_2$/Pentane (d), and 3-$PeONO_2$/Pentane (e). Circles and triangles represent non-smoke and smoke dominated samples collected at Singapore, respectively. Green diamonds show predicted photochemical curves based on zero initial concentrations of RH and $RONO_2$. Dashed red vertical lines are used to mark photochemical ages.

2003; Russo et al., 2010; Swarthout et al., 2013). This signifies the presence of a substantial primary source of $EtONO_2$ at the receptor and/or other formation pathways possibly involving decomposition of larger alkoxy radicals to form ethyl radicals (Bertman et al., 1995; Simpson et al., 2003). Deviations from the predicted curve are comparatively lower, but non-negligible, for 1- and 2-$PrONO_2$ (Fig. 3b and c), echoing previous observations (Bertman et al., 1995; Simpson et al., 2003; Zhou et al., 2005) and suggesting the presence of additional $PrONO_2$ precursors. C_5-$RONO_2$ ratios are evenly distributed around the pure photochemistry curve (Fig. 3d and e), which is expected since n-pentane is the only major precursor of these $RONO_2$ and decomposition of larger radicals do not contribute significantly to levels of alkyl radicals ≥ C_4 in the atmosphere (Bertman et al., 1995).

Further support to the photochemical ages determined using [$RONO_2$/RH] ratios comes from the ratio of propane to ethane (C_3H_8/C_2H_6), which has been used previously to estimate air mass age (Choi et al., 2010). The median C_3H_8/C_2H_6 ratio at the receptor is 0.90, which indicates relatively fresh emissions and is almost midway between values reported for fresh local air (1.2) and fresh regional air (0.57) at a background location in Korea (Choi et al., 2010) and close to that reported for an urban location in Hong Kong (1.2) (Guo et al., 2007).

3.3.2. Clustered air mass backward trajectories

The Hybrid Single-Particle Lagrangian Integrated Trajectory (HYSPLIT) modelling system bundled with Global Data Assimilation System (GDAS) meteorological database is employed for backward trajectory analysis of air parcels to examine the source sectors of SLHs and NMHCs measured at the receptor site. Backward trajectories of air masses at 67 m (height of the sampling location above mean sea level) and 1500 m were analyzed, each with an interval of 3 h for a total duration of 96 h backward. Atwood et al. (2013) have shown that regional biomass burning smoke in SE Asia is often transported above the boundary layer (1000–2000 m) followed by downward-mixing with local urban emissions in Singapore. The 1500 m trajectories are included in the analysis to address this issue. A cluster analysis is then conducted with all computed trajectories using standard HYSPLIT cluster analysis protocol (Stein et al., 2015) in order to elucidate source sectors. By this method, intra-cluster differences between trajectories are minimized while inter-cluster differences are maximized. Computationally, trajectories are combined until the total variance of the individual trajectories about their cluster mean starts to increase substantially (Stunder, 1996). Results of the cluster analysis are presented in Fig. 4.

For the non-smoke dominant samples (n = 143) (Fig. 4a and b), a northeast (NE) and a southeast (SE) cluster are observed for both heights. In addition, the 67 m level shows a northwest (NW) cluster while the 1500 m level shows a west (W) cluster. The SE cluster accounts for the majority of trajectories (54–59%) and represents air masses moving over the Java Sea followed by South Sumatra. This cluster thus represents mixed marine and terrestrial source sectors. The NE cluster (24–27%) is entirely marine and travels over the South China Sea before reaching Singapore. The W cluster for 1500 m and the NW cluster for 67 m (14% and 22%, respectively) mostly represent terrestrial sectors over West and Northwest Sumatra and coastal regions near Singapore.

No cluster analysis is conducted for the smoke-dominant samples because of the low sample number (n = 23); instead, only mean trajectories for each height are shown (Fig. 4c and d). The absence of clustering is not problematic in this case as the overwhelming majority of the trajectories arrive from the SE, especially for the 67 m height, travelling over the Java Sea and then over hotspots in South Sumatra, Jambi and Riau before reaching Singapore. Given the overall similarity between 67 m and 1500 m trajectories, source sectors are analyzed only for the 67 m height level in this paper. Also, trajectory clusters are employed here to mainly study regional emission sources such as marine/terrestrial biogenic activity and peat-forest smoke. For local-scale urban/industrial sources, we use wind sector data from meteorological measurements at the receptor site (see Section 3.4).

3.3.3. Marine and terrestrial biogenic sources

Marine biogenic emission is the major source of species such as DMS, $CHBr_3$, CH_2Br_2 and CH_3Br while terrestrial biogenic emission is a significant additional source of $CHCl_3$, CH_3Cl and CH_3I. The median DMS level in this study (27 pptv) is much lower than values reported in the PEM-Tropics A and B campaigns over the western Pacific (10°N–5°S) (58–75 pptv) (Blake et al., 2003a). DMS exhibits poor correlations with the marine tracers CH_2Br_2 and $CHBr_3$ ($r = 0.22$–0.25, $p < 0.05$) as well as with methyl nitrate ($MeONO_2$) ($r = 0.38$, $p < 0.05$), which is a result of its shorter lifetime as compared to the other tracers. Median DMS values for the marine-dominated NE and SE trajectory sectors are similar (24 and 25 pptv, respectively) while that for the NW sector is slightly lower (21.5 pptv). In addition to marine sources, DMS is also known to be associated with fugitive emissions from natural gas extraction, storage and transport (Swarthout et al., 2013). A low but significant linear correlation ($r = 0.28$, $p < 0.05$) is observed between DMS and the natural gas marker propane (see Section 3.3.4 for possible sources of propane), indicating a possible anthropogenic source of DMS in the study area.

The marine tracers CH_2Br_2 and $CHBr_3$ exhibit median mixing ratios of 1.2 and 3.7 pptv, respectively, which are higher than open ocean values reported from the Pacific, the East and Southeast Asian seas and from the coastal Borneo (Blake et al., 2003a; Zhou et al., 2005 and references therein; Robinson et al., 2014). Atmospheric enrichment of these species near coastal waters (such as Singapore) as compared to open oceans is possibly related to greater coastal abundance of source algae (Yokouchi et al., 1997). These tracers show a moderately good linear correlation ($r = 0.64$, $p < 0.05$) with each other suggesting a common marine source with a median $CH_2Br_2/CHBr_3$ ratio of 0.36, which is much higher than the range (0.14–0.15) reported for fresh coastal emissions near New England, USA and Mace Head, Ireland (Carpenter et al., 2003; Zhou et al., 2005) but similar to values (0.3–0.4) from the Gulf of Mexico and the east coast of USA (Liu et al., 2011). The enhanced ratio in our samples might signify some degree of mixing of coastal air with aged air masses characterized by depleted $CHBr_3$ as reported by Yokouchi et al. (2005b). Further evidence for this is provided by the sectoral distribution of the $CH_2Br_2/CHBr_3$ ratio. The median $CH_2Br_2/CHBr_3$ ratio of 0.53 (highest among the 3 clusters in Fig. 4a and b) for the marine NE sector indicates depletion of $CHBr_3$ in older air masses travelling over the South China Sea. In comparison, for the NW sector, the trajectories mostly originate closer to Singapore over coastal waters in the Malacca and Singapore Straits and exhibit a ratio of 0.15, which is identical to the coastal marine signature reported in the literature (Carpenter et al., 2003; Zhou et al., 2005). The association between CH_2Br_2 and $CHBr_3$ is also enhanced ($r = 0.81$, $p < 0.05$) for the NW sector suggesting co-emission from coastal waters near Singapore.

The median CH_3I mixing ratio for this study (1.2 pptv) is very similar to values reported from other coastal sites across the world (Saiz-Lopez et al., 2012 and references therein) and is enhanced over the background by 147%. The large variation in CH_3I mixing ratios observed in Singapore (mean: 7 ± 19 pptv) with a maximum value of ~141 pptv suggests occasional anthropogenic inputs significantly above the natural background. Oceanic inputs contribute 110–546 Gg y^{-1} to atmospheric CH_3I globally while terrestrial production is estimated to account for 80–110 Gg y^{-1} (Saiz-Lopez et al., 2012 and references therein). Sive et al. (2007) have shown that oceanic and terrestrial fluxes of CH_3I are comparable in magnitude and that the mid-latitude terrestrial biomes contribute 33 Gg y^{-1} to the global CH_3I budget. To distinguish marine contributions from terrestrial inputs, the ratio of CH_3I to the marine tracer $CHBr_3$ is employed (Sive et al., 2007). The median $CH_3I/CHBr_3$ ratio (0.38) in Singapore falls in the terrestrial emissions domain reported by Sive et al. (2007) (0.34 ± 0.27) while closer inspection reveals that only ~10% of the samples fall in the marine emission domain (0.12 ± 0.06). Among trajectory clusters, the lowest median $CH_3I/CHBr_3$ ratio of 0.25 is associated with the NW sector, which is still significantly higher than the reported marine diagnostic ratio. In addition, CH_3I is weakly correlated with the marine tracers CH_2Br_2 ($r = 0.15$, $p > 0.05$) and $CHBr_3$ ($r = 0.30$, $p < 0.05$).

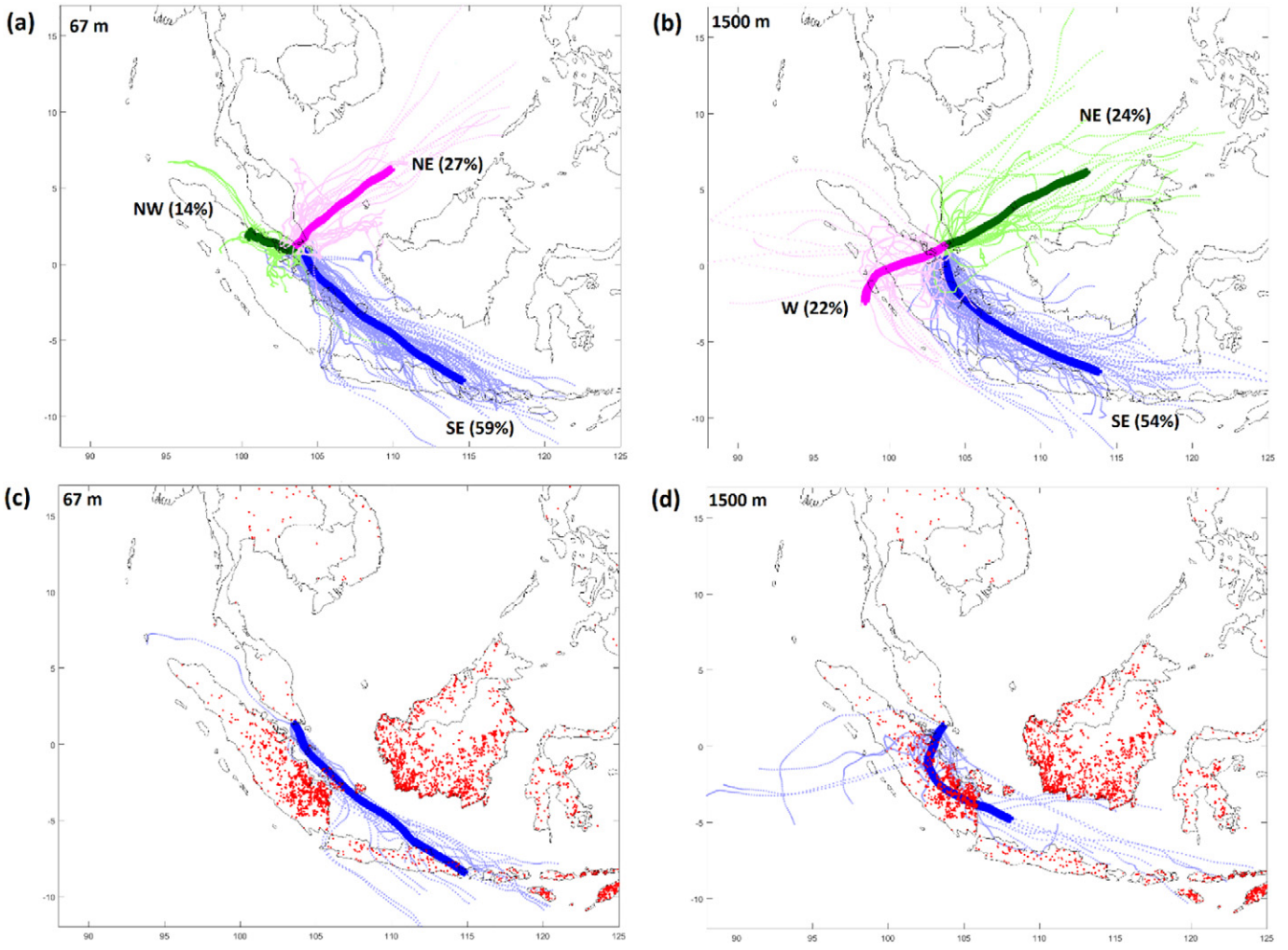

Fig. 4. 96 h HYSPLIT back trajectories and associated clusters for two height levels (67 m and 1500 m) for the non-smoke dominant (a, b; n = 143) and smoke-dominant (c, d; n = 23) samples in Singapore. Clustering of trajectories is described in the text. Dotted lines represent individual trajectories while solid lines represent the mean trajectory for each cluster. MODIS-derived fire hotspots (summed for the observation period) are overlaid for the smoke-dominant category. Only scattered hotspots existed corresponding to individual non-smoke dominant samples; however, these add up to a substantial density when cumulative hotspots for the long observation period (n = 143) is considered. Hotspots for the non-smoke dominant category are not shown to avoid this issue.

Use of a data subset consisting of the bottom 10–20% of CH_3I mixing ratios does not significantly affect the correlations and the median CH_3I/$CHBr_3$ ratio. If samples belonging only to the marine NE sector are considered, the correlation coefficient of CH_3I with $CHBr_3$ increases to 0.76 ($p < 0.05$), revealing oceanic influence. These observations imply that marine influence on CH_3I for a small subset of samples is masked by large local/regional terrestrial sources when the entire suite of samples is considered. Other sources affecting CH_3I levels in Singapore possibly include rice paddies, wetlands, and peat-forest smoke, which are prevalent in the Maritime Continent (Saiz-Lopez et al., 2012).

Marine sources are also known to account for substantial fractions of other SLHs such as $CHCl_3$, CH_3Cl and CH_3Br, and a comparatively smaller fraction (generally, <10%) of CH_2Cl_2. It is important to note here that previous estimates of the marine-derived source of $CHCl_3$ and CH_3Cl have been disputed and it is currently understood that emissions from soils (O'Doherty et al., 2001) and tropical terrestrial vegetation (Hu et al., 2010 and references therein), respectively, are their major global sources. The open ocean acts as an overall sink for CH_3Br, but coastal oceans are considered a significant source (Hu et al., 2010 and references therein; Hu, 2012). Observations from remote coastal areas, open oceans, and marine-dominated air masses in SE Asia have reported mixing ratios in the range of 6–13, 535–675, and 8–10 pptv, respectively, for $CHCl_3$, CH_3Cl and CH_3Br (Blake et al., 2003b; Cox et al., 2003; Low et al., 2003; Simmonds et al., 2004; Guo et al., 2009). In comparison, median mixing ratios of these species observed in Singapore (Table 1) are higher by factors of 1.5–2 and are enriched by 71–204% over corresponding tropospheric backgrounds. This suggests considerable inputs from non-marine sources (see subsequent sections). For the overall dataset (n = 166) as well as for the non-smoke dominated subset (n = 143), $CHCl_3$, CH_3Cl, CH_3Br and CH_2Cl_2 exhibit low correlations with the oceanic tracers CH_2Br_2 ($r = 0.01$–0.26, $p > 0.05$), $CHBr_3$ ($r = -0.08$–0.37, $p > 0.05$) and DMS ($r = 0.10$–0.33, $p > 0.05$). An even smaller subset of samples constrained by the bottom 10% of observed $CHCl_3$ mixing ratios is then considered in order to tease out any underlying marine influence. This exercise significantly improved the correlation of the marine tracer $CHBr_3$ with CH_3Cl ($r = 0.88$, $p < 0.05$), CH_3Br ($r = 0.70$, $p < 0.05$), and CH_3I ($r = 0.66$, $p < 0.05$), while that with CH_2Cl_2 improved by a much smaller amount ($r = 0.40$, $p < 0.05$), thus elucidating the marine-derived components of these halocarbons. These results also indicate that the natural background of these SLHs associated with marine emissions are masked by anthropogenic inputs from local or regional sources.

3.3.4. Industrial sources

Among SLHs, C_2Cl_4 and C_2HCl_3 are sourced entirely from industrial emissions through their use as degreasers, solvents and dry cleaning agents, and are considered vital markers (Guo et al., 2009). The median

mixing ratios of C_2Cl_4 and C_2HCl_3 in Singapore (5.6 pptv for both) are vastly enriched (520–9300%) over background levels but are much lower compared to other urban/industrial areas across the world (Table 1). The correlation between C_2Cl_4 and C_2HCl_3 for the non-smoke dominant dataset ($r = 0.64$, $p < 0.05$) indicates common industrial emissions, while a similar association between these industrial markers and the combustion tracer C_2H_2 ($r = 0.49$ for C_2HCl_3 and $r = 0.71$ for C_2Cl_4; $p < 0.05$) suggests co-located sources.

Among other SLHs, CH_2Cl_2 is emitted primarily from industrial activities via use in paint strippers, degreasers, solvents, chemical feedstock, and foam blowing (WMO, 2010) while CH_3Cl and $CHCl_3$ have partial industrial origins in the form of solvent and feedstock use (Chan and Chu, 2007; Guo et al., 2009). In view of the short atmospheric lifetimes of these species (Table S1, Supplementary material), their high median enhancements over the global baseline (~90–1500%, Table 1) indicates continuous emission inputs in Singapore and from neighboring countries. Long-term aircraft measurements (1998–2012) have revealed steadily increasing levels (by 7–15 pptv, depending on the location) of atmospheric CH_2Cl_2, possibly as a consequence of increased usage in the production of HFC-32, a replacement refrigerant, in the post-MP era (Leedham Elvidge et al., 2015). For the non-smoke dominant dataset, CH_2Cl_2 shows moderate correlation with the industrial tracers C_2Cl_4 ($r = 0.37$, $p < 0.05$) and C_2HCl_3 ($r = 0.53$, $p < 0.05$), suggesting the presence of a common source in the form of industrial solvents and degreasers related to chemical, pharmaceutical and electronics industries. The correlation between $CHCl_3$ and CH_2Cl_2 ($r = 0.66$, $p < 0.05$) suggests an industrial solvent use source for $CHCl_3$ as well; this is further supported by its correlations with C_2Cl_4 ($r = 0.31$, $p < 0.05$) and C_2HCl_3 ($r = 0.50$, $p < 0.05$). This industrial source of $CHCl_3$ could therefore mask its marine signature, as discussed in Section 3.3.3. Levels of CH_3Cl, on the other hand, are poorly correlated with the industrial markers C_2HCl_3 and C_2Cl_4 ($r = 0.03$–0.11), which points towards the presence of a biomass burning source as discussed in the next section.

Among SLHs, CH_3Br deserves special attention as an ODS. The median CH_3Br mixing ratio in Singapore of 21 pptv is 204% of the tropospheric background, and 11–61% higher compared to PRD and Hong Kong (Table 1), indicating continuous inputs to the atmosphere. These inputs could be in the form of biomass burning emissions (see next section), use in agricultural fumigation, and/or quarantine and pre-shipment (QPS) applications (Li et al., 2014). QPS applications are allowed for all MP signatory countries. Industrial production of CH_3Br was phased-out as per the MP by 1998 in most developed nations while Article 5 signatories agreed to freeze CH_3Br use for agricultural fumigation in 2002, followed by 20% reduction in 2005 and a complete phase-out in 2015. In fact, many developing countries (e.g., Indonesia) committed to achieve the phase-out well before MP deadlines (UNEP, 1999). Since detailed usage data of CH_3Br as a fumigating agent from neighboring countries with substantial agricultural activities (i.e., Malaysia and Indonesia) are not available, more information is needed to assess the importance of agriculture-related sources on the levels of CH_3Br observed at our study site. Based on available information (NEA, 2016), Singapore froze the consumption of CH_3Br for non-quarantine and pre-shipment applications in 2002 followed by phase-out starting 1 January 2015. Hence, in the absence of sustained emissions from other regional consumers, the atmospheric abundances of CH_3Br in this region are likely to reduce sharply in the near future owing to its short atmospheric lifetime of 0.7 years.

3.3.5. Peat-forest burning sources

To aid in investigating the potential impacts of peat-forest burning smoke on levels of SLHs such as $CHCl_3$, CH_2Cl_2, CH_3Cl, CH_3Br and CH_3I, we employ selected NMHCs (ethane, ethyne, propane, and benzene) and CO. Ethyne and CO are widely used as tracers for combustion emissions (Swarthout et al., 2013) and show reasonable correlation ($r = 0.57$ for the entire dataset; $r = 0.61$ for the non-smoke dominant subset; $p < 0.05$). The most significant source of propane in urban areas is the use of liquefied petroleum gas (LPG) with a minor fraction from vehicle exhausts, while that for ethane and benzene are natural gas leakage, and vehicular exhausts and industrial solvent use, respectively (Simpson et al., 2010; Gilman et al., 2013). These potentially interfering sources must be considered prior to utilizing these NMHCs to track biomass burning impacts. The median i-butane/n-butane ratio at the receptor site (0.43) indicates leakage from domestic LPG use, with only ~10% of samples each in the vehicular exhaust (0.2–0.3) and natural gas (0.6–1.0) domains (Simpson et al., 2010). The good correlation of propane with the butanes ($r = 0.73$–0.74, $p < 0.05$) supports its major source of LPG usage. The propane/ethyne ratio (median: 1.1) suggests an additional industrial source of propane related to natural gas processing and use as solvent (Gilman et al., 2013 and references therein), which is expected given the presence of petrochemical facilities in the study area. Ethane, on the other hand, shows poorer correlations with the butanes ($r = 0.32$–0.49, $p < 0.05$) and propane ($r = 0.57$, $p < 0.05$), and is enriched over propane (median ethane/propane: 1.1). Considering that ethane is generally a minor constituent of natural gas/LPG, such enrichments presumably result from biomass burning inputs in a subset of samples (see below). Lastly, while the overall toluene/benzene ratio (median: 2.1) is close to vehicle exhaust signature, a substantial fraction of samples (~35%) are affected by emissions from industrial solvent use with ratios >3 (Yurdakul et al., 2013).

Observed mixing ratios of SLHs and NMHCs in samples collected near peat-forest fires in Riau, Indonesia (n = 8) are presented in Table S4 (Supplementary material). Riau samples exhibit exceedingly high median mixing ratios, on the order of a few tens of ppbv to a few ppmv, for the SLHs (except $CHCl_3$) and NMHCs, showing massive releases from peat and associated biomass burning. However, $CHCl_3$ levels (median: 64 pptv) were only slightly enhanced in near-source samples, indicating a minor contribution from biomass burning. SLHs measured at Riau show good correlations with benzene ($0.70 < r < 0.89$, $p < 0.05$), ethyne ($0.34 < r < 0.83$, $p < 0.05$) and propane ($0.61 < r < 0.97$, $p < 0.05$) but not with ethane ($-0.24 < r < 0.32$). The presence of a local ethane source of substantial magnitude might cause this lack of correlation, but we are not aware of such a source and are not able to explain this observation. Only 3 valid CO measurements were possible in the near-source samples while the remaining 5 samples were off-scale. Despite the limitations mentioned above, CO and ethane, rather than ethyne, measurements are selectively used here to characterize peat fire emissions. This is done for two reasons: i) using ratios relative to CO and ethane enables us to compare our results with those from previous biomass burning campaigns (BIBLE A, TRACE-A, and TRACE-P); and ii) CO and ethane are mostly associated with smoldering combustion, which is a characteristic of the peat fires of interest in this study, while ethyne is emitted in larger proportions from flaming fires (Lobert et al., 1991).

For the near-source samples, the median CO/CO_2 ratio of 0.23 (range: 0.15–0.27) suggests smoldering combustion (Blake N.J. et al., 1996) typical of peat fires in SE Asia. Ratios of SLHs and NMHCs relative to CO (pptv/ppbv) are then calculated and compared with other biomass burning measurements conducted previously (Table 2). The median ratio of CH_3Cl/CO (0.69) for the near-source samples falls within the range (0.54–0.85) reported for South American agricultural burning and African savannah emissions in the TRACE-A campaign (Blake N.J. et al., 1996) and SE Asian air masses in the TRACE-P campaign (Blake et al., 2003b) while those for CH_3Br/CO (0.021) and CH_3I/CO (0.012) are higher than reported values. In comparison, ratios of ethane, ethyne, propane and benzene to CO (2.1, 0.15, 0.64 and 0.44, respectively) are much lower than reported ranges for TRACE-A and TRACE-P (Blake N.J. et al., 1996, 2003b). It is noted that species with the highest ratios relative to CO (CH_3Cl, ethane, propane and benzene, Table 2) are mostly associated with smoldering combustion (Lobert et al., 1991) and are good candidates to evaluate the impacts of smoldering peat fires. Ratios of SLHs and NMHCs relative to ethane (pptv/pptv) were then computed (Table 2) and it was observed that near-source CH_3Cl/ethane, CH_3Br/ethane and CH_3I/ethane ratios of 0.4, 0.01 and 0.008 are higher by factors of 4–

Table 2
Median ratios of selected short-lived halocarbons (SLHs) and non-methane hydrocarbons (NMHCs) relative to CO and ethane measured near peat-forest fires in Riau, Indonesia and in Singapore. Also provided are ratios reported for TRACE-A, TRACE-P and BIBLE A campaigns (Blake N.J. et al., 1996, 2003b; Elliott et al., 2003). Ratios relative to CO are given as pptv/ppbv while those relative to ethane are given as pptv/pptv.

Ratio	Near-source (Riau)	Receptor (Singapore)	TRACE-A[a]	TRACE-P[a,b]	BIBLE A
CH_3Cl/CO	0.69	3.24	0.57–0.85	0.54	
CH_3Br/CO	0.021	0.067	0.006–0.011	0.006	
CH_3I/CO	0.012	0.005	0.0012		
Ethane/CO	2.09	6.59	5.2–8.3	5.5	
Ethyne/CO	0.15	1.61	3.3–4.5	4.0	
Propane/CO	0.64	4.66	0.97–1.6	1.0	
Benzene/CO	0.44	4.92	1.29–1.30		
CH_3Cl/ethane	0.41	0.48			0.10
CH_3Br/ethane	0.014	0.012			0.001
CH_3I/ethane	0.008	0.001			0.0001–0.001
Ethyne/ethane	0.15	0.81			0.50
Propane/ethane	0.31	0.74			0.25
Benzene/ethane	0.27	0.30			0.40

[a] Emission ratios were calculated as the slope of individual linear regressions of SLHs and NMHCs with respect to CO.
[b] Values are for the SE Asian air mass.

10 compared to values referenced and reported in the BIBLE A campaign (Elliott et al., 2003). Among NMHCs, propane exhibits a slightly higher ratio (0.31) than reported (0.25) while those for ethyne and benzene are lower by factors of 1.5–3.

Since the sample collection in Riau (December 2011) did not overlap with that in Singapore, a direct correspondence between near-source and receptor data in terms of plume transport cannot be established. Nevertheless, a numerical exercise is conducted based on source-to-receptor transport times and atmospheric lifetimes of selected species (neglecting mixing and dilution) to study the effects on observed ratios. Based on trajectory analysis, a 1 day transport time from Riau to Singapore is considered. Individual ratios of $CHCl_3$, CH_3Cl and CH_3Br relative to CO, ethane, ethyne and benzene for near-source samples are allowed to undergo atmospheric processing via reactions with OH radical using the integrated form of the rate law for a pseudo-first order reaction. A 12 h daytime average concentration of 2.0×10^6 molecule cm^{-3} is assumed for OH radical in troposphere (Atkinson and Arey, 2003). For CH_3I, photolysis is considered to be the dominant atmospheric reaction pathway and an overall lifetime of 4 days is assumed. The largest changes because of transport (7–12% depletion) are observed for ratios of CH_3I with the NMHCs and CO, while for the rest of SLHs, the variation is within 1–5%. This shows that for the short transport time from Riau to Singapore, SLH/NMHC ratios are conserved with respect to OH radical induced reactions.

Mixing ratios of SLHs, NMHCs and CO for non-smoke dominant and smoke-dominant periods in Singapore are presented in Table 3. Only one trajectory cluster exists for the smoke-dominant samples (Section 3.3.2 and Fig. 4c), and observed levels of all species discussed here are associated with trajectories originating in the SE sector, travelling over fire spots in South Sumatra prior to reaching Singapore. First, it is noted that median mixing ratios of CH_2Cl_2 and $CHCl_3$ are lower on smoke-dominant days as compared to non-smoke dominant ones. This, when coupled with the small enrichment in near-source samples, confirms that transported peat-forest smoke is not a significant source of $CHCl_3$ at the receptor site. In the absence of near-source data for CH_2Cl_2, its associations with other biomass burning tracers in receptor samples are studied. For the smoke-dominant samples, CH_2Cl_2 correlates poorly with CH_3Cl, CO, ethane, propane and benzene ($-0.13 < r < 0.16$) but strongly with the industrial markers toluene ($r = 0.67$, $p < 0.05$) and C_2HCl_3 ($r = 0.92$, $p < 0.05$), and the combustion tracer ethyne ($r = 0.57$, $p < 0.05$). This implies a primarily industrial rather than biomass burning-related origin of CH_2Cl_2 in Singapore. This is supported by previous field measurements reporting overestimation of CH_2Cl_2 in biomass burning plumes (Simpson et al., 2011).

Next, it is observed that mixing ratios of the remaining SLHs, NMHCs and CO in Singapore are higher by ~10–60% in the presence of transboundary smoke (Table 3), with ethane, benzene and CH_3I showing the highest enrichments. Among methyl halides, only CH_3Cl shows a reasonable correlation with CO on smoke-dominant days ($r = 0.61$, $p < 0.05$) while CH_3Br shows a low association ($r = 0.36$, $p > 0.05$) and CH_3I is uncorrelated ($r = 0.04$). These SLHs show only moderate associations ($0.25 < r < 0.53$) with ethane, propane and benzene, possibly because of substantial background emissions of these NMHCs from local sources as discussed previously. Among NMHCs, the ethane/propane ratio for the smoke-dominant subset of samples (median: 1.4) is enhanced compared to the median for the entire dataset (1.1), showing additional ethane inputs to the urban atmosphere in the presence of peat-forest smoke. Similarly, the toluene/benzene ratio is close to the biomass burning domain (median: 1.2) for this subset suggesting enhanced emissions of benzene from peat-forest fires.

Lastly, SLH and NMHC ratios relative to CO and ethane observed at the receptor are compared to those measured near fire sources in Riau (Table 2). It is noted that the ratios of CH_3Cl, CH_3Br and benzene relative to ethane are remarkably close to those measured at Riau and are in agreement with negligible modification during transport. The CH_3I/ethane ratio is depleted by a factor of ~8 as compared to near-source samples, possibly because of the short atmospheric lifetime of CH_3I. Most other ratios at the receptor, especially those of NMHCs relative to CO, are significantly enriched compared to both near-source and literature values. This most likely results from the substantial and variable background levels of NMHCs and some SLHs in the urban environment of Singapore. In addition, atmospheric mixing and dilution during transport and individual species lifetimes can disproportionately affect ratios and cause large variations, as observed in Table 2. It will be worthwhile if future studies from this region are designed to systematically target these issues.

Table 3
Comparison between non-smoke-dominant and smoke dominant mixing ratios of selected halocarbons (pptv), NMHCs (pptv), and CO (ppbv) in Singapore. Also shown are percent change between median mixing ratios of each species for the two categories.

Species	Non-smoke dominant (n = 143)		Smoke-dominant (n = 23)		% change
	Mean ± 1σ	Median	Mean ± 1σ	Median	
CH_2Cl_2	338 ± 743	91	379 ± 889	84	−8
CH_3Cl	964 ± 280	889	1055 ± 256	992	+12
$CHCl_3$	36 ± 43	19	18 ± 12	13	−32
CH_3Br	31 ± 38	21	33 ± 27	24	+14
CH_3I	7 ± 20	1.2	3 ± 6	1.7	+42
C_2H_6	1655 ± 925	1500	2756 ± 1692	2425	+62
C_2H_2	1545 ± 1832	1166	2161 ± 1594	1280	+10
C_3H_8	1728 ± 1468	1382	2296 ± 1800	1596	+15
C_6H_6	558 ± 600	412	784 ± 498	607	+47
CO	262 ± 96	238	381 ± 210	292	+23

Overall, the receptor and near-source observations coupled with photochemical aging and air mass transport described in this section suggest – i) emissions from local urban/industrial sources such as domestic LPG use, natural gas processing, vehicular traffic and solvent use contribute to a significant urban background for NMHCs; ii) the possibility of substantial dilution/loss of SLHs during atmospheric transport from fire source regions to Singapore, to the point that the very strong fire-related SLH and NMHC signatures near the source can be masked by the urban-industrial signatures at the receptor; and iii) ethane, CO, benzene, ethyne and, to some extent, propane, CH_3Cl and CH_3I, show impacts of transported peat-forest smoke on a subset of samples. $CHCl_3$ and CH_2Cl_2, on the other hand, appear mostly to be related to industrial emissions and show minor enhancements from peat-forest smoke.

3.4. Association of halocarbons with wind sector data

While backward trajectories can be helpful in understanding regional source sectors, they might not be able to provide similar insights on much smaller scales such as an urban environment with various industrial clusters. To this end, binned (45°) wind sector data from co-located meteorological measurements at the sampling site are used along with similarly binned halocarbon data to identify sectors of high abundance (Fig. 5). Unlike the rest of this paper, mean halocarbon data are used in this exercise instead of median in order to capture sectors associated with occasional extreme values. The dominant wind direction for the study period is from the south (median: 183°). Among halocarbons, CFCs show an even distribution of mixing ratios across all wind sectors (Fig. 5a) which is expected for species with residual atmospheric background levels rather than localized inputs dependent on particular source sectors. The same is true for other phased-out species such as halons, CCl_4 and CH_3CCl_3 (not shown). For halocarbons that are in use, two distinct trends are seen. Levels of C_2HCl_3, C_2Cl_4 and CH_2Cl_2 that are primarily used in industrial applications as solvents, cleaning agents, feedstock material and degreasers (Table S1, Supplementary material) show peaks for the W-NW sector (Fig. 5c and d), potentially associated with emissions from chemical and petrochemical industries. Species such as HFC-134a, HCFC-22 and HCFC-141b, on the other hand, exhibit transient high values associated mostly with the E-SE sector followed by a smaller peak in the W-NW sector (Fig. 5b). These are potentially associated with refrigerant and polymer production in industrial clusters coupled with island-wide emissions from domestic refrigeration and automobile air conditioning (especially for HFC-134a) that possibly contribute towards attenuating a clear directional gradient. The CH_3Br peak is related to the W-NW sector (Fig. 5c) as a possible consequence of cargo fumigation in ports.

3.5. Quantitative source apportionment with PMF

PMF-derived sources profiles and mean source contributions are provided in Table 4 based on a 9-factor solution with satisfactory agreement between modeled and measured total gases ($R^2 = 0.86$, $p < 0.01$). These results are adopted to discuss the potential sources of halocarbons in Singapore during 2011–2012.

Source 1 (Residual refrigeration): this source is dominated by CFCs with high mass percentages of CFC-11 (80%), CFC-12 (59%) and CFC-113 (41%), which indicates residual levels from refrigerant production in the pre-MP era (Zhang et al., 2010).

Source 2 (Secondary formation): this source is characterized by $RONO_2$ (60–85%) and is indicative of atmospheric oxidation processes leading to the formation of these alkyl nitrates from parent alkanes.

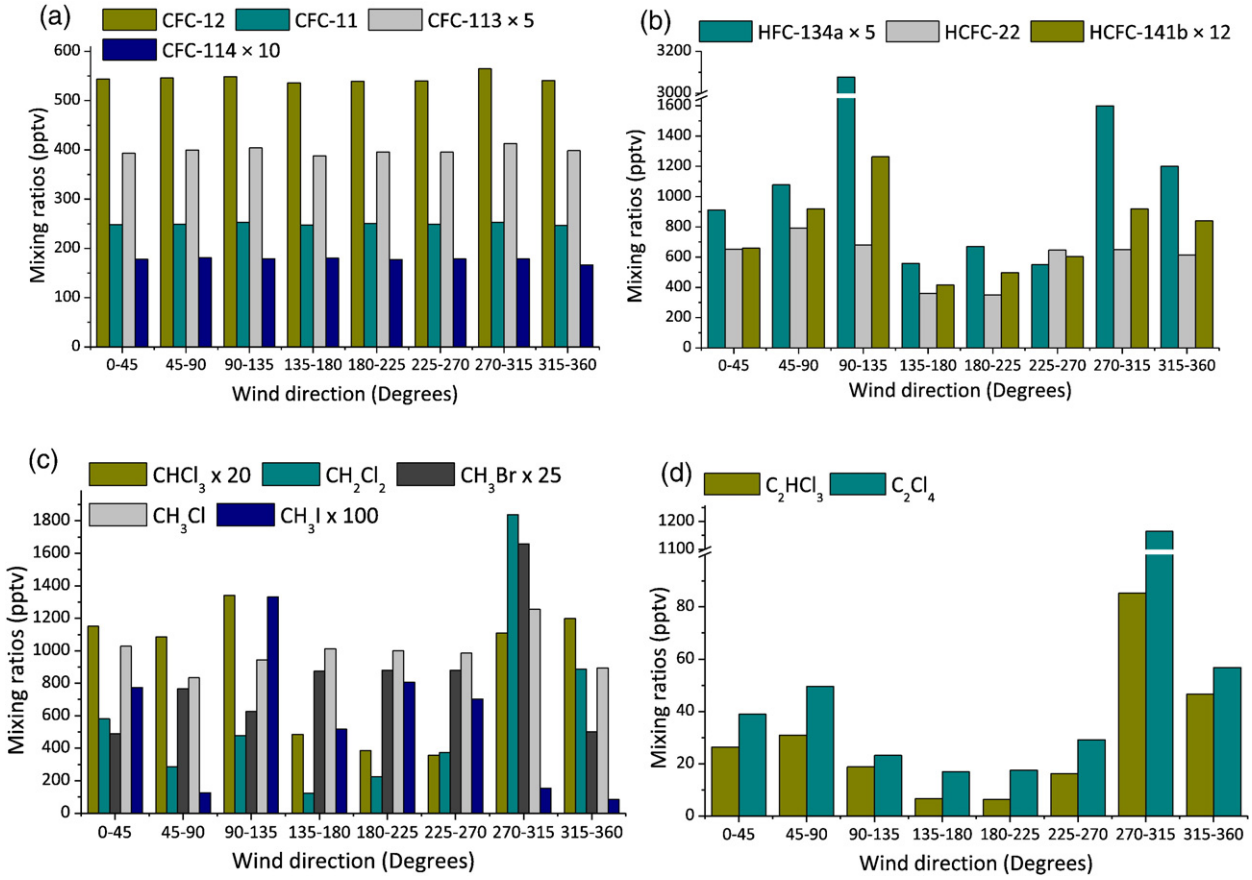

Fig. 5. Variation of selected halocarbon mixing ratios (pptv) for observed wind sectors in Singapore during Aug–Oct 2011–2012. Halocarbon data are classified into 45° wind bins. Individual plots show: dependence of mixing ratios on wind sectors for CFCs (a); HFC-134a, HCFC-22 and HCFC1-141b (b); $CHCl_3$, CH_2Cl_2, CH_3Br, CH_3Cl and CH_3I (c); CH_3CCl_3 and C_2Cl_4 (d). Note that certain halocarbon mixing ratios are multiplied by factors of 5–100 to aid representation.

Table 4
Source profiles of halocarbons, NMHCs and other gases (pptv; calculated as enhancements) in Singapore determined from the chosen 9-factor solution of PMF. Numbers in parentheses represent percentages of each species associated with individual sources.

Species	Residual refrigeration	Secondary formation	Industry	Marine/terrestrial biogenic	Marine biogenic	Peat-forest smoke	Residual solvent	LPG/natural gas	Fumigation
CO	6741.4 (5)	0.0 (0)	16,230.0 (13)	24,550.0 (19)	12,743.0 (10)	67,400.0 (53)	0.0 (0)	0.0 (0)	0.0 (0)
DMS	0.0 (0)	0.0 (0)	3.0 (16)	8.2 (44)	3.5 (19)	0.0 (0)	1.6 (8)	2.3 (12)	0.0 (0)
CFC-12	8.0 (59)	0.0 (0)	0.8 (6)	0.0 (0)	0.0 (0)	0.0 (0)	4.4 (32)	0.0 (0)	0.3 (2)
CFC-11	9.4 (80)	0.4 (4)	0.1 (1)	0.6 (5)	0.2 (2)	0.0 (0)	0.0 (0)	0.0 (0)	1.0 (8)
CFC-113	1.7 (41)	0.2 (6)	0.5 (13)	0.2 (4)	0.0 (0)	0.0 (0)	0.9 (22)	0.0 (0)	0.5 (13)
HFC-134a	1.2 (4)	0.0 (0)	26.4 (85)	0.3 (1)	0.0 (0)	0.0 (0)	0.0 (0)	0.0 (0)	3.0 (10)
HCFC-22	1.3 (1)	1.5 (1)	163.6 (80)	16.3 (8)	0.0 (0)	0.0 (0)	9.3 (5)	7.7 (4)	4.8 (2)
CH_3CCl_3	0.01 (2)	0.0 (0)	0.1 (11)	0.1 (17)	0.0 (0)	0.0 (0)	0.4 (59)	0.1 (11)	0.0 (0)
CCl_4	1.3 (17)	0.04 (1)	0.3 (3)	1.0 (13)	0.5 (7)	0.0 (0)	3.8 (49)	0.3 (4)	0.5 (6)
CH_2Cl_2	0.3 (1)	1.3 (3)	24.3 (64)	0.0 (0)	10.5 (28)	0.4 (1)	0.0 (0)	1.3 (3)	0.0 (0)
C_2HCl_3	0.2 (7)	0.3 (12)	2.0 (70)	0.1 (3)	0.02 (1)	0.0 (0)	0.1 (5)	0.1 (2)	0.0 (0)
C_2Cl_4	0.0 (0)	0.3 (7)	2.3 (64)	0.0 (0)	0.3 (8)	0.0 (0)	0.2 (4)	0.3 (9)	0.3 (8)
CH_3Cl	19.0 (5)	0.4 (0)	19.9 (5)	145.6 (39)	23.7 (6)	88.3 (23)	54.8 (15)	0.0 (0)	26.0 (7)
CH_3Br	0.0 (0)	0.0 (0)	0.4 (2)	0.5 (3)	0.6 (3)	2.8 (15)	0.9 (5)	0.0 (0)	13.2 (72)
CH_3I	0.0 (0)	0.04 (6)	0.0 (0)	0.2 (28)	0.0 (0)	0.5 (67)	0.0 (0)	0.0 (0)	0.0 (0)
CH_2Br_2	0.004 (1)	0.04 (14)	0.0 (0)	0.1 (18)	0.2 (53)	0.0 (0)	0.03 (11)	0.01 (2)	0.0 (0)
$CHBr_3$	0.1 (2)	0.2 (6)	0.0 (0)	0.4 (9)	2.9 (76)	0.0 (0)	0.0 (0)	0.0 (0)	0.2 (6)
$EtONO_2$	0.0 (0)	0.8 (60)	0.0 (0)	0.0 (0)	0.1 (7)	0.2 (17)	0.2 (16)	0.0 (0)	0.0 (0)
1-$PrONO_2$	0.3 (6)	3.5 (61)	0.0 (0)	0.0 (0)	0.1 (2)	1.1 (20)	0.6 (10)	0.0 (0)	0.1 (1)
2-$PrONO_2$	0.0 (0)	0.3 (60)	0.01 (1)	0.0 (0)	0.0 (0)	0.1 (16)	0.1 (23)	0.0 (0)	0.0 (0)
2-$BuONO_2$	0.5 (6)	6.4 (75)	0.1 (2)	0.4 (5)	0.0 (0)	0.7 (8)	0.1 (1)	0.3 (3)	0.0 (0)
3-$PeoNO_2$	0.1 (1)	4.0 (83)	0.1 (1)	0.4 (8)	0.0 (0)	0.04 (1)	0.0 (0)	0.1 (1)	0.2 (5)
2-$PeONO_2$	0.0 (0)	6.2 (85)	0.1 (2)	0.7 (9)	0.2 (2)	0.0 (0)	0.1 (1)	0.0 (0)	0.0 (0)
Ethane	42.6 (4)	39.5 (4)	0.0 (0)	0.0 (0)	35.9 (4)	591.7 (59)	25.8 (3)	181.9 (18)	80.7 (8)
Ethyne	0.0 (0)	6.8 (1)	42.4 (8)	0.0 (0)	106.0 (21)	208.1 (41)	0.0 (0)	145.4 (29)	0.0 (0)
Propane	25.2 (2)	80.1 (6)	13.6 (1)	56.8 (4)	0.0 (0)	164.0 (13)	0.0 (0)	821.4 (65)	106.5 (8)
i-Butane	14.0 (2)	39.2 (6)	53.0 (8)	29.8 (4)	33.5 (5)	0.0 (0)	6.5 (1)	489.9 (72)	15.0 (2)
n-Butane	0.0 (0)	87.1 (5)	125.4 (7)	107.1 (6)	0.0 (0)	0.0 (0)	40.5 (2)	1303.5 (74)	99.7 (6)
Benzene	0.0 (0)	4.1 (1)	22.3 (8)	0.0 (0)	62.8 (21)	131.7 (45)	0.0 (0)	72.9 (25)	0.0 (0)
Toluene	0.0 (0)	0.0 (0)	251.7 (47)	0.0 (0)	53.9 (10)	11.0 (2)	15.4 (3)	207.9 (39)	0.0 (0)
Total halocarbons	42.5 (6)	4.9 (1)	240.8 (34)	165.2 (23)	38.9 (5)	92.0 (13)	74.8 (10)	9.8 (1)	49.8 (7)

Source 3 (Industry): this source is an amalgamation of emissions from various industrial activities. The presence of high mass fractions of HFC-134a and HCFC-22 (85% and 80%, respectively) suggest impacts from the production of refrigeration and foam blowing replacements, and mobile air conditioning applications (McCulloch et al., 2003; Chan and Chu, 2007). This source also includes signatures of industrial solvent use with high mass percentages of C_2HCl_3 (70%), CH_2Cl_2 (64%), C_2Cl_4 (64%) and toluene (47%), which are widely used as solvents, degreasers and feedstock in chemical (plastic, pharmaceutical, and others) and electronics industries.

Source 4 (Marine/Terrestrial biogenic): this source profile is characterized by DMS (44%), CH_3Cl (39%), CH_3I (28%) and CH_2Br_2 (18%). Marine biogenic sources of DMS and CH_2Br_2, especially in coastal waters, are well known (Yokouchi et al., 1997) while possible marine and terrestrial sources of CH_3I and CH_3Cl at the study location have been discussed in Section 3.3.3.

Source 5 (Marine biogenic): this source is represented by oceanic tracers $CHBr_3$ (76%) and CH_2Br_2 (53%), and a small amount of DMS (19%). This source profile also contains a non-trivial mass fraction (~28%) of CH_2Cl_2. A small marine signature of CH_2Cl_2 has been indicated in Section 3.3.3. With regard to Sources 4 and 5, the PMF analysis is not able to provide a clear quantitative distinction between marine and terrestrial sources of these SLHs in the present scenario. A potential reason might be that most air masses arriving at the receptor travel over both oceanic and land sectors causing intermixing of marine and terrestrial signatures (see Section 3.3.2).

Source 6 (Peat-forest smoke): this source is dominated by large mass percentages of CH_3I (67%), ethane (59%), CO (53%), benzene (45%) and ethyne (41%). This profile is consistent with observations of halocarbon and NMHC abundances and associations from near-source and receptor samples as discussed previously. Small fractions of CH_3Cl (23%), CH_3Br (15%) and propane (13%), and a negligible fraction of CH_2Cl_2 (~1%) are found to be associated with this transported peat-forest smoke, which supports the suggestions made in Section 3.3.5.

Source 7 (Residual solvent): high mass percentages of CH_3CCl_3 (59%) and CCl_4 (49%) make up this source profile with some contributions from CFC-12 (32%) and CFC-113 (23%) as well. This indicates legacy levels from industrial solvent use and degreasing (Chan and Chu, 2007) in the pre-MP period.

Source 8 (LPG/Natural gas): this source profile is loaded primarily with n-butane (74%), i-butane (72%) and propane (65%), with a much lower contribution from ethane (29%). This clearly indicates leakage from domestic LPG use and emissions from natural gas processing in the urban environment as suggested in Section 3.3.4. It is noted that this source also includes moderate amounts of toluene (39%) and benzene (25%), which are potential by-products of natural gas extraction and processing. Emissions of benzene and toluene from natural gas extraction processes have been reported previously (Marrero et al., 2016; Rich and Orimoloye, 2016).

Source 9 (Fumigation): this source is characterized by a large mass percentage of CH_3Br (72%), and is possibly related to fumigation for QPS applications (Li et al., 2014). The insignificant loadings of marine/terrestrial biogenic and biomass burning tracers in this factor also support this source assignment.

Based on this PMF analysis, halocarbons in the atmosphere of Singapore are emitted mostly from industrial sources (34%), which include the use of industrial solvents, degreasers, refrigerant production and foam blowing, among others. The next largest source is marine/terrestrial biogenic activity that contributes 28%, followed by residual levels of solvents and refrigerants from the pre-MP era (16%), seasonal influxes of transboundary peat-forest smoke (13%), and QPS fumigation (7%). Overall, these PMF results are consistent with those from previous analyses described in Sections 3.3.3–3.3.5. This is especially the case for marine/terrestrial biogenic, peat-forest smoke, industrial, and LPG/natural gas

emission sources, for which PMF-derived source profiles and contributions closely mirror the indications from sector-wise abundances, interspecies correlations and diagnostic ratios.

3.6. Limitations and future prospects

It is appropriate here to outline some limitations of the present study and briefly discuss the prospects for future work. First, this study utilized samples collected only during the SW monsoon season in Singapore (i.e., Aug–Oct) and therefore was not able to investigate seasonal variations, if any, in source strengths. Incorporating year-round sample collection would enhance the understanding of seasonal variations at the study site. Second, given the preliminary interpretation of sources responsible for halocarbon loadings observed in this study, corresponding near-source sampling could be carried out in the future to verify individual source signatures. Third, because of the absence of publicly available halocarbon emission inventories for the study site, it was not possible to validate PMF-derived source estimates from this study with sector-wise inventory data. Such inventory data, if available, would also help in differentiating emissions into production- and consumption-related categories. Fourth, future studies should ideally extend atmospheric halocarbon measurements to determine top-down emission estimates followed by comparisons with bottom-up emission inventories. And fifth, results from this study stress the importance of designing future campaigns by collecting comparable and correlated samples near peat-forest fire sites and in receptor locations in order to study evolution of SLH distributions as a function of plume transport.

4. Conclusions

An intensive sampling campaign was conducted in Singapore spanning August–October of 2011–2012 to study, for the first time, levels and sources of tropospheric halocarbons in this region. The results were analyzed in the context of regional production and usage patterns of halocarbons and applicable international and national regulatory frameworks. Four major conclusions are drawn from the study as described below.

First, Singapore's implementation of Montreal Protocol regulations on the import and use of ODS ahead of schedule (mid-1990s) has resulted in significant reductions in their levels. Measured levels of ODS such as CFCs, halons, CCl_4 and CH_3CCl_3 in Singapore are only marginally higher (1–17%) than the global tropospheric background and are comparable to those at remote locations.

Second, following the CFC phase-out, first- and second-generation CFC replacements such as HCFCs and HFCs have emerged as the dominant halocarbon species in Singapore. Among these, HCFC-22, HCFC-141b and HFC-134a are the most prevalent with atmospheric enhancements of 39–67% over global backgrounds. This observation is supported by the regional usage pattern of these species as refrigerants, aerosol propellants and foam blowing agents. Major consumers in the SE Asian region (i.e., Singapore, Indonesia and Malaysia) have started implementing HCFC phase-out management plans since 2012–13. This addresses, in a timely fashion, environmental concerns stemming from the considerably high atmospheric levels and the large GWPs for some of these species.

Third, emissions from LPG leakage, natural gas operations and industrial solvent use contribute to a substantial urban baseline for non-methane hydrocarbons such as ethane, propane, and benzene thereby masking to some extent their signatures from transboundary peat-forest fires. For short-lived halocarbons, CH_2Cl_2 and $CHCl_3$ appear to be sourced mostly from industrial emissions while CH_3I, CH_3Cl and CH_3Br are related in varying proportions to marine, terrestrial biogenic, peat-forest fire and fumigation sources. The strong signatures of these halocarbons in near-source samples are potentially affected by atmospheric mixing/dilution during transport and by mixing with regional background levels at the receptor site.

Fourth, a PMF analysis of the available dataset revealed that industrial emissions from a variety of sectors are responsible for 34% of the observed halocarbon loadings in Singapore. The natural background of short-lived halocarbons derived from marine and terrestrial biogenic activity contributes 28% while residual levels of ODS (CFCs, halons, CCl_4, and CH_3CCl_3) from pre-Montreal Protocol operations contribute 16%. Seasonal incidences of transboundary peat-forest smoke in the Maritime Continent account for 13% of observed halocarbons. These estimates, especially for industrial sources, should be considered provisional until verified by sector-wise emission inventories.

Acknowledgement

The authors thank the anonymous reviewers for their detailed and constructive comments, and numerous helpful suggestions. The authors wish to thank NASA-MIT Advanced Global Atmospheric Gases Experiment (AGAGE) (www.agage.mit.edu) and Earth System Research Laboratory (ESRL) of the National Oceanic and Atmospheric Administration (NOAA) (www.esrl.noaa.gov) for halocarbon tropospheric background data. The authors also thank Prof. Matthias Roth (Department of Geography, NUS) for providing meteorological data at the sampling site. The analysis of canister samples at Donald Blake's lab was financially supported by NASA, USA. Jeffrey Reid's participation was funded by the Naval Research Laboratory Base Research Program. Seed funding provided by the provost office (R706-000-032-133) at the National University of Singapore is appreciated.

Appendix A. Supplementary data

Supplementary data to this article can be found online at https://doi.org/10.1016/j.scitotenv.2017.11.087.

References

AFEAS, 2006. Alternative Fluorocarbons Environmental Acceptability Study. Available online at. https://agage.mit.edu/data/afeas-data.

Artuso, F., Chamard, P., Chiavarini, S., di Sarra, A., Meloni, D., Piacentino, S., Sferlazzo, M.D., 2010. Tropospheric halocompounds and nitrous oxide monitored at a remote site in the Mediterranean. Atmos. Environ. 44, 4944–4953.

Atkinson, R., Arey, J., 2003. Atmospheric degradation of volatile organic compounds. Chem. Rev. 103, 4605–4638.

Atwood, S.A., Reid, J.S., Kreidenweis, S.M., Yu, L.E., Salinas, S.V., Chew, B.N., Balasubramanian, R., 2013. Analysis of source regions for smoke events in Singapore for the 2009 El Nino burning season. Atmos. Environ. 78, 219–230.

Bertman, S.B., Roberts, J.M., Parrish, D.D., Buhr, M.P., Goldan, P.D., Kuster, W.C., Fehsenfeld, F.C., Montzka, S.A., Westberg, H., 1995. Evolution of alkyl nitrates with air mass age. J. Geophys. Res. 100, 22805–22813.

Blake, D.R., Chen, T.Y., Smith, T.W., Wang, C.J.L., Wingenter, O.W., Blake, N.J., Rowland, F.S., Mayer, E.W., 1996a. Three dimensional distribution of nonmethane hydrocarbons and halocarbons over the northwestern Pacific during the 1991 Pacific Exploratory Mission (PEM-West A). J. Geophys. Res. 101, 1763–1778.

Blake, N.J., Blake, D.R., Sive, B.C., Chen, T.Y., Rowland, F.S., Collins, J.E., Sachse, G.W., Anderson, B.E., 1996b. Biomass burning emissions and vertical distribution of atmospheric methyl halides and other reduced carbon gases in the South Atlantic region. J. Geophys. Res. 101, 24151–24164.

Blake, N.J., Blake, D.R., Chen, T.Y., Collins, J.E., Sachse, G.W., Anderson, B.E., Rowand, F.S., 1997. Distribution and seasonality of selected hydrocarbons and halocarbons over the western Pacific basin during PEM-West A and PEM-West B. J. Geophys. Res. 102, 28315–28331.

Blake, N.J., Blake, D.R., Swanson, A.L., Atlas, E., Flocke, F., Rowland, F.S., 2003a. Latitudinal, vertical and seasonal variations of C_1-C_4 alkyl nitrates in the troposphere over the Pacific Ocean during PEM-Tropics A and B: oceanic and continental sources. J. Geophys. Res. 108 (D2), 8242.

Blake, N.J., Blake, D.R., Simpson, I.J., Meinardi, S., Swanson, A.L., Lopez, J.P., Katzenstein, A.S., Barletta, B., Shirai, T., Atlas, E., 2003b. NMHCs and halocarbons in Asian continental outflow during the Transport and Chemical Evolution over the Pacific (TRACE-P) Field Campaign: comparison with PEM-West B. J. Geophys. Res. 108 (D20), 8806.

Butler, J.H., Yvon-Lewis, S.A., Lobert, J.M., King, D.B., Montzka, S.A., Bullister, J.L., Koropalov, V., Elkins, J.W., Hall, B.D., Hu, L., Liu, Y., 2016. A comprehensive estimate for loss of atmospheric carbon tetrachloride (CCl_4) to the ocean. Atmos. Chem. Phys. 16, 10899–10910.

Carpenter, L.J., Liss, P.S., Penkett, S.A., 2003. Marine organohalogens in the atmosphere over the Atlantic and Southern Oceans. J. Geophys. Res. 108 (D9), 4256.

Chan, L.Y., Chu, K.W., 2007. Halocarbons in the atmosphere of the industrial-related Pearl River Delta region of China. J. Geophys. Res. 112, D04305. https://doi.org/10.1029/2006JD007097.

Choi, Y., Elliott, S., Simpson, I.J., Blake, D.R., Colman, J.J., Dubey, M.K., Meinardi, S., Rowland, F.S., Shirai, T., Smith, F.A., 2003. Survey of whole air data from the second airborne Biomass Burning and Lightning Experiment using principal component analysis. J. Geophys. Res. 108 (D5), 4163.

Choi, E., Heo, J.B., Yi, S.M., 2010. Apportioning and locating nonmethane hydrocarbon sources to a background site in Korea. Environ. Sci. Technol. 44, 5849–5854.

Cox, M.L., Sturrock, G.A., Fraser, P.J., Siems, S., Krummel, P.B., O'Doherty, S., 2003. Regional sources of methyl chloride, chloroform and dichloromethane identified from AGAGE observations at Cape Grim, Tasmania, 1998–2000. J. Atmos. Chem. 45, 79–99.

Department of Statistics, 2016. Yearbook of Statistics Singapore 2016. Department of Statistics, Singapore Government, Singapore www.singstat.gov.sg.

Elliott, S., Blake, D.R., Blake, N.J., Dubey, M.K., Rowland, F.S., Sive, B.C., Smith, F.A., 2003. BIBLE A whole-air sampling as a window on Asian biogeochemistry. J. Geophys. Res. 108 (D3), 8407.

ESRL, 2016. The Halocarbons and Other Atmospheric Trace Species (HATS) Dataset. Earth System Research Laboratory (ESRL), National Oceanic and Atmospheric Administration (NOAA) Available online at. www.esrl.noaa.gov/gmd/hats/.

Fang, X., Wu, J., Su, S., Han, J., Wu, Y., Shi, Y., Wan, D., Sun, X., Zhang, J., Hu, J., 2012. Estimates of major anthropogenic halocarbon emissions from China based on interspecies correlations. Atmos. Environ. 62, 26–33.

Gilman, J.B., Lerner, B.M., Kuster, W.C., de Gouw, J.A., 2013. Source signature of volatile organic compounds from oil and natural gas operations in northeastern Colorado. Environ. Sci. Technol. 47, 1297–1305.

Graziosi, F., Arduini, J., Bonasoni, P., Furnali, F., Giostra, U., Manning, A.J., McCulloch, A., O'Doherty, S., Simmonds, P.G., Reimann, S., Vollmer, M.K., Maione, M., 2016. Emissions of carbon tetrachloride from Europe. Atmos. Chem. Phys. 16, 12849–12859.

Guo, H., So, K.L., Simpson, I.J., Barletta, B., Meinardi, S., Blake, D.R., 2007. C_1-C_8 volatile organic compounds in atmosphere of Hong Kong: overview of atmospheric processing and source apportionment. Atmos. Environ. 41, 1456–1472.

Guo, H., Ding, A.J., Wang, T., Simpson, I.J., Blake, D.R., Barletta, B., Meinardi, S., Rowland, F.S., Saunders, S.M., Fu, T.M., Hung, W.T., Li, Y.S., 2009. Source origins, modeled profiles, and apportionments of halogenated hydrocarbons in the greater Pearl River Delta region, southern China. J. Geophys. Res. 114, D11302. https://doi.org/10.1029/2008JD011448.

Hu, L., 2012. The Role of the Ocean in the Atmospheric Budgets of Methyl Bromide, Methyl Chloride and Methane. Ph.D. dissertation. Texas A&M University, Texas, USA.

Hu, L., Yvon-Lewis, S.A., Liu, Y., Salisbury, J.E., O'Hern, J.E., 2010. Coastal emissions of methyl bromide and methyl chloride along the eastern Gulf of Mexico and the east coast of the United States. Glob. Biogeochem. Cycles 24, GB1007.

Hu, L., Montzka, S.A., Miller, B.R., Andrews, A.E., Miller, J.B., Lehman, S.J., Sweeney, C., Miller, S.M., Thoning, K., et al., 2016. Continued emissions of carbon tetrachloride from the United States nearly two decades after its phaseout for dispersive uses. Proc. Natl. Acad. Sci. 113, 2880–2885.

Hurst, D.F., Lin, J.C., Romashkin, P.A., Daube, B.C., Gerbig, C., Matross, D.M., Wofsy, S.C., Hall, B.D., Elkins, J.W., 2006. Continuing global significance of emissions of Montreal Protocol-restricted halocarbons in the United States and Canada. J. Geophys. Res. 111, D15302. https://doi.org/10.1029/2005JD006785.

IPCC/TEAP, de Jager, D., 2005. IPCC/TEAP special report on safeguarding the ozone layer and the global climate system: issues related to hydrofluorocarbons and perfluorocarbons. In: Metz, B., Kuijpers, L., Solomon, S., Andersen, S.O., Davidson, O., Pons, J., Kestin, T., Manning, M., Meyer, L.A. (Eds.), Working I and III of the Intergovernmental Panel on Climate Change, and the Technology and Economic Assessment Panel. Cambridge University Press, Cambridge, United Kingdom and New York, NY, USA.

Keller, C.A., Hill, M., Vollmer, M.K., Henne, S., Brunner, D., Reimann, S., O'Doherty, S., Arduini, J., Maione, M., Ferenczi, Z., Haszpra, L., Manning, A.J., Peter, T., 2012. European emissions of halogenated greenhouse gases inferred from atmospheric measurements. Environ. Sci. Technol. 46, 217–225.

Khan, M.A.H., Mead, M.I., White, I.R., Golledge, B., Nickless, G., Knights, A., Martin, D., Rivett, A.C., Greally, B.R., Shallcross, D.E., 2009. Year-long measurements of C1-C3 halocarbons at an urban site and their relationship with meteorological parameters. Atmos. Sci. Lett. 10, 75–86.

Kim, K.-H., Shon, Z.-H., Nguyen, H.T., Jeon, E.-C., 2011. A review of major chlorofluorocarbons and their halocarbon alternatives in the air. Atmos. Environ. 45, 1369–1382.

Kurylo, M.J., Rodriguez, J.M., Andreae, M.O., Atlas, E.L., Blake, D.R., Butler, J.H.S., Lary, D.J., Midgeley, P.M., Montzka, S.A., Novelli, P.C., Reeves, C.E., Simmonds, P.G., Steele, P.L., Sturges, W.T., Weiss, R.F., Yokouchi, Y., 1999. Short-lived ozone-related compounds, chap. 2 in scientific assessment of ozone depletion: 1998. WMO Global Ozone Research and Monitoring Project Report No. 44, pp. 2.1–2.56.

Lan, Y., Sarkar, S., Jia, S., Tham, J., Yap, W.L., Fan, W.H., Reid, J.S., Sng, J., Ong, C.N., Yu, L.E., 2017. Long-term observations of the effects of transboundary peat-forest smoke on an urban environment in Southeast Asia (Manuscript in preparation).

Leedham Elvidge, E.C., Oram, D.E., Laube, J.C., Baker, A.K., Montzka, S.A., Humphrey, S., O'Sullivan, D.A., Brenninkmeijer, C.A.M., 2015. Increasing concentrations of dichloromethane, CH_2Cl_2, inferred from CARIBIC air samples collected 1998–2012. Atmos. Chem. Phys. 15, 1939–1958.

Li, S., Kim, J., Park, S., Kim, S.-K., Park, M.-K., Muhle, J., Lee, G., Lee, M., Jo, C.O., Kim, K.-R., 2014. Source identification and apportionment of halogenated compounds observed at a remote site in East Asia. Environ. Sci. Technol. 48, 491–498.

Li, Z., Bie, P., Wang, Z., Zhang, Z., Jiang, H., Xu, W., Zhang, J., Hu, J., 2016. Estimated HCFC-22 emissions for 1990–2050 in China and the increasing contributions to global emissions. Atmos. Environ. 132, 77–84.

Liu, Y., Yvon-Lewis, S.A., Hu, L., Salisbury, J.E., O'Hern, J.E., 2011. $CHBr_3$, CH_2Br_2 and $CHClBr_2$ in U.S. coastal waters during the Gulf of Mexico and East Coast Carbon cruise. J. Geophys. Res. 116, C10004.

Lobert, J.M., Scharffe, D.H., Hao, W.M., Kuhlbusch, T.A., Seuwen, R., Warneck, P., Crutzen, P.J., 1991. Experimental evaluation of biomass burning emissions: Nitrogen and carbon containing compounds. In: Levine, J.S. (Ed.), Global Biomass Burning - Atmospheric, Climatic, and Biospheric Implications. MIT Press, Cambridge, USA.

Low, J.C., Wang, N.Y., Williams, J., Cicerone, R.J., 2003. Measurements of ambient atmospheric C_2H_5Cl and other ethyl and methyl halides at coastal California sites and over the Pacific Ocean. J. Geophys. Res. 108 (D19), 4608.

Marrero, J.E., Townsend-Small, A., Lyon, D.R., Tsai, T.R., Meinardi, S., Blake, D.R., 2016. Estimating emissions of toxic hydrocarbons from natural gas production sites in the Barnett Shale Region of Northern Texas. Environ. Sci. Technol. 50, 10756–10764.

McCulloch, A., Midgley, P.M., Ashford, P., 2003. Releases of refrigerant gases (CFC-12, HCFC-22 and HFC-134a) to the atmosphere. Atmos. Environ. 37, 889–902.

NEA, 2012. Hydrochlorofluorocarbons (HCFCs) Phase-out Management Plan in Singapore. NEA Dialogue Session, 8th October 2012. National Environment Agency, Singapore Government, Singapore.

NEA, 2016. Control of Ozone Depleting Substances. National Environment Agency, Singapore Government, Singapore Available online at. http://www.nea.gov.sg/anti-pollution-radiation-protection/chemical-safety/multilateral-environmental-agreements/ozone-depleting-substances.

O'Doherty, S., Simmonds, P.G., Cunnold, D.M., Wang, H.J., Sturrock, G.A., Fraser, P.J., Ryall, D., Derwent, R.G., Weiss, R.F., Salameh, P., Miller, B.R., Prinn, R.G., 2001. In situ chloroform measurements at Advanced Global Atmospheric Gases Experiment atmospheric research stations from 1994 to 1998. J. Geophys. Res. 106, 20429–20444.

O'Doherty, S., Cunnold, D.M., Manning, A., Miller, B.R., Wang, R.H.J., Krummel, P.B., Fraser, P.J., Simmonds, P.G., McCulloch, A., Weiss, R.F., Salameh, P., Porter, L.W., Prinn, R.G., Huang, J., Sturrock, G., Ryall, D., Derwent, R.G., Montzka, S.A., 2004. Rapid growth of hydrofluorocarbon 134a and hydrochlorofluorocarbons 141b, 142b, and 22 from Advanced Global Atmospheric Gases Experiment (AGAGE) observations at Cape Grim, Tasmania, and Mace Head, Ireland. J. Geophys. Res. 109, D06310. https://doi.org/10.1029/2003JD004277.

Palmer, P.I., Jacob, D.J., Mickley, L.J., Blake, D.R., Sachse, G.W., Fuelberg, H.E., Kiley, C.M., 2003. Eastern Asian emissions of anthropogenic halocarbons deduced from aircraft concentration data. J. Geophys. Res. 108 (D24):4753. https://doi.org/10.1029/2003JD003591.

Prinn, R.G., Weiss, R.F., Krummel, P.B., O'Doherty, S., Fraser, P.J., Muhle, J., Reimann, S., Vollmer, M.K., Simmonds, P.G., Maione, M., Arduini, J., Lunder, C.R., Schmidbauer, N., Young, D., Wang, H.J., Huang, J., Rigby, M., Harth, C.M., Salameh, P.K., Spain, T.G., Steele, L.P., Arnold, T., Kim, J., Hermansen, O., Derek, N., Mitrevski, B., Langenfelds, R., 2016. The ALE/GAGE AGAGE Network. Carbon Dioxide Information Analysis Center (CDIAC), Oak Ridge National Laboratory (ORNL), U.S. Department of Energy (DOE).

Reimann, S., Vollmer, M.K., Folini, D., Steinbacher, M., Hill, M., Buchmann, B., Zander, R., Mahieu, E., 2008. Observations of long-lived anthropogenic halocarbons at the high-Alpine site of Jungfraujoch (Switzerland) for assessment of trends and European sources. Sci. Total Environ. 391, 224–231.

Rich, A.L., Orimoloye, H.T., 2016. Elevated atmospheric levels of benzene and benzene-related compounds from unconventional shale extraction and processing: human health concern for residential communities. Environ. Health Insights 10, 75–82.

Roberts, J.M., Bertman, S.B., Parrish, D.D., Fehsenfeld, F.C., Jobson, T., Niki, H., 1998. Measurement of alkyl nitrates at Chebogue Point, Nova Scotia during the 1993 North Atlantic Regional Experiment (NARE) intensive. J. Geophys. Res. 103, 13569–13580.

Robinson, A.D., Harris, N.R.P., Ashfold, M.J., Gostlow, B., Warwick, N.J., O'Brien, L.M., Beardmore, E.J., Nadzir, M.S.M., Phang, S.M., Samah, A.A., Ong, S., Ung, H.E., Peng, L.K., Yong, S.E., Mohamad, M., Pyle, J.A., 2014. Long-term halocarbon observations from a coastal and an inland site in Sabah, Malaysian Borneo. Atmos. Chem. Phys. 14, 8369–8388.

Russo, R.S., Zhou, Y., Haase, K.B., Wingenter, O.W., Frinak, E.K., Mao, H., Talbot, R.W., Sive, B.C., 2010. Temporal variability, sources, and sinks of C_1-C_5 alkyl nitrates in coastal New England. Atmos. Chem. Phys. 10, 1865–1883.

Saikawa, E., Rigby, M., Prinn, R.G., Montzka, S.A., Miller, B.R., Kuijpers, L.J.M., Fraser, P.J.B., Vollmer, M.K., et al., 2012. Global and regional emission estimates for HCFC-22. Atmos. Chem. Phys. 12, 10033–10050.

Saiz-Lopez, A., Plane, J.M.C., Baker, A.R., Carpenter, L.J., von Glasow, R., Gomez Martin, J.C., McFiggans, G., Saunders, R.W., 2012. Atmospheric chemistry of iodine. Chem. Rev. 112, 1773–1804.

Shao, M., Huang, D., Gu, D., Lu, S., Chang, C., Wang, J., 2011. Estimate of anthropogenic halocarbon emission based on measured ratio relative to CO in the Pearl River Delta region, China. Atmos. Chem. Phys. 11, 5011–5025.

Simmonds, P.G., Derwent, R.G., Manning, A.J., Fraser, P.J., Krummel, P.B., O'Doherty, S.O., Prinn, R.J., Cunnold, D.M., et al., 2004. AGAGE observations of methyl bromide and methyl chloride at Mace Head, Ireland and Cape Grim, Tasmania, 1998–2001. J. Atmos. Chem. 47, 243–269.

Simpson, I.J., Blake, N.J., Blake, D.R., Atlas, E., Flocke, F., Crawford, J.H., Fuelberg, H.E., Kiley, C.M., Meinardi, S., Rowland, F.S., 2003. Photochemical production and evolution of C_2-C_5 alkyl nitrates in tropospheric air influences by Asian outflow. J. Geophys. Res. 108 (D20), 8808.

Simpson, I.J., Blake, N.J., Barletta, B., Diskin, G.S., Fuelberg, H.E., Gorham, K., Huey, L.G., Meinardi, S., Rowland, F.A., Vay, S.A., Weinheimer, A.J., Yang, M., Blake, D.R., 2010. Characterization of trace gases measured over Alberta oil sands mining operations: 76 speciated C_2–C_{10} volatile organic compounds (VOCs), CO_2, CH_4, CO, NO, NO_2, NO_y, O_3 and SO_2. Atmos. Chem. Phys. 10, 11931–11954.

Simpson, I.J., Akagi, S.K., Barletta, B., Blake, N.J., Choi, Y., Diskin, G.S., Fried, A., Fuelberg, H.E., Meinardi, S., Rowland, F.S., Vay, S.A., Weinheimer, A.J., Wennberg, P.O., Wiebring, P., Wisthaler, A., Yang, M., Yokelson, R.J., Blake, D.R., 2011. Boreal forest fire emissions in fresh Canadian smoke plumes: C_1-C_{10} volatile organic compounds (VOCs), CO_2, CO, NO_2, NO, HCN and CH_3CN. Atmos. Chem. Phys. 11, 6445–6463.

Sive, B.C., Varner, R.K., Mao, H., Blake, D.R., Wingenter, O.W., Talbot, R., 2007. A large terrestrial source of methyl iodide. Geophys. Res. Lett. 34, L17808.

SPARC, 2016. SPARC report on the mystery of carbon tetrachloride. In: Liang, Q., Newman, P.A., Reiman, S. (Eds.), SPARC Report No. 7, WCRP/13, 2016.

Stein, A.F., Draxler, R.R., Rolph, G.D., Stunder, B.J.B., Cohen, M.D., Ngan, F., 2015. NOAA's HYSPLIT atmospheric transport and dispersion modelling system. Bull. Am. Meteorol. Soc. https://doi.org/10.1175/BAMS-D-14-00110.1.

Stohl, A., Seibert, P., Arduini, J., Eckhardt, S., Fraser, P., Greally, B.R., Lunder, C., Maione, M., Muhle, J., O'Doherty, S., Prinn, R.G., Reimann, S., Saito, T., Schmidbauer, N., Simmonds, P.G., Vollmer, M.K., Weiss, R.F., Yokouchi, Y., 2009. An analytical inversion method for determining regional and global emissions of greenhouse gases: sensitivity studies and application to halocarbons. Atmos. Chem. Phys. 9, 1597–1620.

Stohl, A., Kim, J., Li, S., O'Doherty, S., Salameh, P.K., Saito, T., Vollmer, M.K., Wan, D., Yao, B., Yokouchi, Y., Zhou, L.X., 2010. Hydrochlorofluorocarbon and hydrofluorocarbon emissions in East Asia determined by inverse modelling. Atmos. Chem. Phys. 10, 2089–2129.

Stunder, B.J.B., 1996. An assessment of the quality of forecast trajectories. J. Appl. Meteorol. 35, 1319–1331.

Swarthout, R.F., Russo, R.S., Zhou, Y., Hart, A.H., Sive, B.C., 2013. Volatile organic compound distributions during the NACHTT campaign at the Boulder Atmospheric Observatory: influence of urban and natural gas sources. J. Geophys. Res. Atmos. 118, 10614–10637.

UNDP, 2012. HCFC Phase-out Management Plan (HPMP) Stage-I for Compliance with the 2013 and 2015 Control Targets for Annex-C, Group-I Substances (HCFCs) in Malaysia. United Nations Development Programme Project Document.

UNEP, 1999. Methyl Bromide Phase-out Strategies: A Global Compilation of Laws and Regulations. United Nations Environment Programme Division of Technology, Industry and Economics (UNEP TIE) Available online at. www.unepie.org/ozonaction.html.

UNEP, 2011. Project Proposal: Indonesia. United Nations Environment Programme: Executive Committee of the Multilateral Fund for the implementation of the Montreal Protocol, 64th Meeting, Montreal, 25–29 July 2011.

US EPA, 2014. EPA Positive Matrix Factorization (PMF) 5.0 Fundamentals and User Guide. United States Environmental Protection Agency, Washington, DC, USA.

Vollmer, M.K., Zhou, L.X., Greally, B.R., Henne, S., Yao, B., Reimann, S., Stordal, F., Cunnold, D.M., Zhang, X.C., Maione, M., Zhang, F., Huang, J., Simmonds, P.G., 2009. Emissions of ozone-depleting halocarbons from China. Geophys. Res. Lett. 36, L15823. https://doi.org/10.1029/2009GL038659.

WMO, 2010. Scientific Assessment of Ozone Depletion: 2010. Global Ozone Research and Monitoring Project – Report No. 52. World Meteorological Organization, Geneva, Switzerland.

WMO, 2014. Scientific Assessment of Ozone Depletion: 2014. Global Ozone Research and Monitoring Project – Report No. 55. World Meteorological Organization, Geneva, Switzerland.

Wu, J., Fang, X., Martin, J.W., Zhai, Z., Su, S., Hu, X., Han, J., Lu, S., Wang, C., Zhang, J., Hu, J., 2014. Estimated emissions of chlorofluorocarbons, hydrochlorofluorocarbons, and hydrofluorocarbons based on an interspecies correlation method in the Pearl River Delta region, China. Sci. Tot. Environ. 470–471, 829–834.

Yokouchi, Y., Mukai, H., Yamamoto, H., Otsuki, A., Saitoh, C., Nojiri, Y., 1997. Distribution of methyl iodide, ethyl iodide, bromoform, and dibromomethane over the ocean (east and southeast Asian seas and the western Pacific). J. Geophys. Res. 102 (D7), 8805–8809.

Yokouchi, Y., Inagaki, T., Yazawa, K., Tamaru, T., Enomoto, T., Izumi, K., 2005a. Estimates of ratios of anthropogenic halocarbon emissions from Japan based on aircraft monitoring over Sagami Bay, Japan. J. Geophys. Res. 110, D06301. https://doi.org/10.1029/2004JD005320.

Yokouchi, Y., Hasebe, F., Fujiwara, M., Takashima, H., Shiotani, M., Nishi, N., Kanaya, Y., Hashimoto, S., Fraser, P., Toom- Sauntry, D., Mukai, H., Nojiri, Y., 2005b. Correlations and emission ratios among bromoform, dibromochloromethane, and dibromomethane in the atmosphere. J. Geophys. Res. Atmos. 110, D23309.

Yokouchi, Y., Nojiri, Y., Toom-Sauntry, D., Fraser, P., Inuzuka, Y., Tanimoto, H., Nara, H., Murakami, R., Mukai, H., 2012. Long-term variation of atmospheric methyl iodide and its link to global environmental change. Geophys. Res. Lett. 39, L23805.

Yurdakul, S., Civan, M., Tuncel, G., 2013. Volatile organic compounds in suburban Ankara atmosphere, Turkey: sources and variability. Atmos. Res. 120-121, 298–311.

Zhang, Y.L., Guo, H., Wang, X.M., Simpson, I.J., Barletta, B., Blake, D.R., Meinardi, S., Rowland, F.S., Cheng, H.R., Saunders, S.M., Lam, S.H.M., 2010. Emission patterns and spatiotemporal variations of halocarbons in the Pearl River Delta region, southern China. J. Geophys. Res. 115, D15309. https://doi.org/10.1029/2009JD013726.

Zhang, Y., Wang, X., Simpson, I.J., Barletta, B., Blake, D.R., Meinardi, S., Louie, P.K.K., Zhao, X., Shao, M., Zhong, L., Wang, B., Wu, D., 2014. Ambient CFCs and HCFC-22 observed concurrently at 84 sites in the Pearl River Delta region during the 2008–2009 grid studies. J. Geophys. Res. Atmos. 119, 7699–7717.

Zhou, Y., Varner, R.K., Russo, R.S., Wingenter, O.W., Haase, K.B., Talbot, R., Sive, B.C., 2005. Coastal water source of short-lived halocarbons in New England. J. Geophys. Res. 110, D21302.